Univerzita Karlova v Praze

Matematicko-fyzikální fakulta

DIPLOMOVÁ PRÁCE

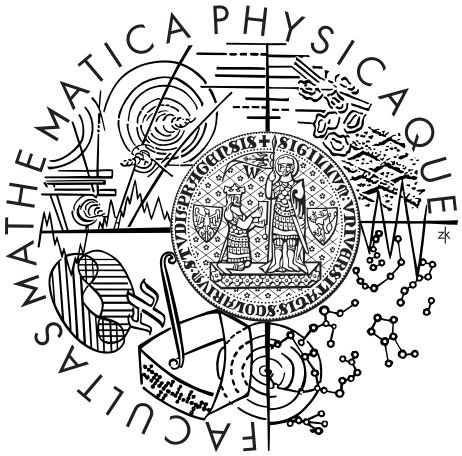

Jana Lipková

Stochastické modelování reakčně-difuzních procesů v biologii

Matematicko-fyzikální fakulta

Vedoucí diplomové práce: prof. RNDr. Bohdan Maslowski DrSc.

Studijní program: Matematika

Studijní obor: matematické modelování ve fyzice a technice

Praha 2011

I would like to thank my supervisor prof. RNDr. Bohdan Maslowski for the opportunity to write this thesis and also prof. RNDr. Josef Málek for opportunity to learn mathematics applied to field of biology from the best as he promised when I was considering mathematical modelling department. He was very right. I would like to thank Dr. Konstantinos Zygalakis, Dr. Mark Flegg for their support and motivation and especially Dr. Radek Erban for his kind guidance and mentoring and without whom this thesis would not happen. It was my honour to collaborate with them. Finally I would like to thank Michal Dzian and Ondrej Tichý for their help with many small things that helped to complete this work.

Prohlašuji, že jsem tuto diplomovou práci vypracoval(a) samostatně a výhradně s použitím citovaných pramenů, literatury a dalších odborných zdrojů.

Beru na vědomí, že se na moji práci vztahují práva a povinnosti vyplývající ze zákona č. 121/2000 Sb., autorského zákona v platném znění, zejména skutečnost, že Univerzita Karlova v Praze má právo na uzavření licenční smlouvy o užití této práce jako školního díla podle §60 odst. 1 autorského zákona.

V ..... dne ..... Podpis autora

Název práce: Stochastické modelování reakčně-difuzních procesů v biologii

Autor: Jana Lipková

Katedra: Matematicko-fyzikální fakulta

Vedoucí diplomové práce: prof. RNDr. Bohdan Maslowski, DrSc.
Katedra pravděpodobnosti a matematické statistiky

Abstrakt: Mnoho biologických procesov sa dá popísať pomocou chemických reakcií a difúzie. Táto práca študuje reakčne-difúzne mechanizmy v spojení s vytváraním Turingových vzorov. Odvodené sú postačujúce a nutné podmienky pre vznik turingovej nestability. Správanie sa turingových vzorov je skúmané deterministickým prístupom, priehradkovou stochastickou simuláciou (compartment-based SSA) a molekulovou stochastickou simuláciou (molecular-based SSA).

Klíčová slova: reakčne-difuzné processy, Turinové vzory, stochastické modelovanie

Title: On Stochastic Modelling of Reaction-Diffusion Processes in Biology

Author: Jana Lipková

Department: Faculty of Mathematics and Physics

Supervisor: prof. RNDr. Bohdan Maslowski, DrSc.
Department of Probability and Mathematical Statistics

Abstract: Many biological processes can be described in terms of chemical reactions and diffusion. In this thesis, reaction-diusion mechanisms related to the formation of Turing patterns are studied. Necessary and sufficient conditions under which Turing instability occur is presented. Behaviour of Turing patterns is investigated with a use of deterministic approach, compartment-based stochastic simulation algorithm and molecular-based stochastic simulation algorithm.

Keywords: reaction-diffusion processes, Turing patterns, stochastic modelling

Contents

1. Introduction

In this work we study biological processes which can be described in terms of reaction and diffusion. In particular, we consider a system of components whose state is modified by chemical reactions and whose movement is governed by diffusion. Processes described by these mechanisms play an important role in biology. The applications of reaction-diffusion processes are both numerous and diverse. We have included an overview of a few of specific examples below.

A well known reaction-diffusion process is pattern formation. In 1952, Alan Turing, the same man who deciphered the Enigma code, suggested that under certain conditions chemicals can react and diffuse in such a way as to produce spatial patterns. Nearly 40 years after the Turing hypothesis, the experimental evidence of patterns was discovered. Pattern formation mechanisms have been used to describe many different phenomena, such as pigmentation patterning in mammalian coat [1] or the pattern formation of follicles in the skin of mice [12]. Moreover, they play an important role in developmental biology and embryology.

Another example of application can be found in bacteriology. For instance reaction-diffusion mechanisms participate in a signal transduction in *E. coli* chemotaxis [15, 47, 48]. Bacterial chemotaxis is a movement of bacteria in response to changes in extracellular signal molecules. Thanks to this, bacteria can find food by swimming towards the highest concentration of food molecules, or avoid noxious environment. The transformation of the signal from receptors at the bacterial membrane to motors governing its movement occurs through signalling pathways. This process is called signalling transduction.

D. Fange and J. Elf [16] used a reaction-diffusion model to model the division of *E.Coli* . These elongated bacteria divide symmetrically in two parts to ensure that both newly formed daughter cells contain a copy of the chromosome. The symmetry of the division is ensured by so called Min proteins. They oscillate back and forth between the cell poles to help the parental bacterium find its middle before cell division.

In a recent model, reaction-diffusion mechanisms were used to simulate signalling pathways of mitogen-activated protein kinases (MAPKs) [13]. MAPKs are enzymes that are involved in a wide range of cellular processes such as the regulation of gene expression, mitosis[1], cell differentiation, and proliferationCell proliferation is the increase in cell number as a result of cell growth and division., but also

[1]Mitosis is a process of cell division which results in the production of two daughter cells from a single parent cell. The daughter cells are identical to one another and to the original parent cell.

program cell death[2]. The MAPK signalling pathway is a chain of proteins in the cell that transfers a signal from a receptor on the surface of the cell to the DNA in the nucleus of the cell. A mutation of any protein in this pathway is an initial step in the development of many cancers. Drugs that reverse these mutations are investigated as cancer treatments [14].

1.1 Mathematical Modelling of Reaction-Diffusion Processes

A traditional approach for the simulation of reaction diffusion processes is to characterize each chemical species by its concentration and then describe the time evolution of these concentrations by a system of partial differential equations (PDEs). An advantage of this deterministic approach is that for solving and modelling of PDEs we can choose from extensive set of analytical and numerical tools [6, 21].

However, the situation is much more delicate when we take into account biological systems. In this case, there may be relatively low number of some chemical species; for instance often only one or two mRNA molecules of a particular gene are presented in a cell [22]. In such a situation, we cannot properly define concentration and thus the deterministic models become inaccurate. Instead of concentrations, we characterize the system by the number and position of molecules and instead of continuum-based deterministic models we will use discrete stochastic models [6]. Thus, the stochastic-based models provide a much more detailed description of the system as their deterministic opposites do. In this thesis we study two stochastic simulation algorithms (SSAs) for chemical reactions.

From the molecular point of view, we can intuitively accept the fact that chemical reactions involving two or more reactants occur when reacting molecules collide. It means molecules that are separated by a smaller distance have a higher chance to react as remote molecules. On the other hand, not each collision need to be necessary followed by reaction. This is caused by reaction-activation energy. Sometimes molecules can react, only if they collide in a certain way, for instance if corresponding sites on the surface of molecules meet[1, 26]. This is incorporated in both presented SSAs by assigning a certain probability to the occurrence of chemical reactions.

The first presented SSA, belongs to the class of *Compartment-based models* [6, 54]. As the name suggests, in this approach we divide the domain in imaginary com-

[2]The term programmed cell death was introduced in 1964, proposing that cell death during development is not of accidental nature but follows a sequence of controlled steps leading to locally and temporally defined self-destruction [52].

partments. To simulate chemical reactions, it is postulated that only molecules within the same compartment may react. Diffusion is then modelled as a jump process between neighbour compartments [6]. This approach is used in the RD simulator [23, 46].
The second presented SSA belong in the class of *Molecular-based models*. Here we assume that particles evolve according to Brownian motion. Diffusion is then described by a system of stochastic differential equations. Diffusing molecules can collide only if their centres are separated by the distance less then the sum of their radii. If this is the case, then the chemical reactions occurs with certain probability [5, 6, 7]. A variant of this approach is used in Smoldyn package [34, 36].

This dissertation is ordered as follows. In Chapter 2, we explain modelling of the chemical reactions in well-stirred system, using the deterministic and the stochastic approach. Then, in Chapter 3, we focus on a special reaction-diffusion mechanism, the formation of Turing pattern. We present necessary and sufficient conditions under which reaction-diffusion processes produce Turing patterns. Interesting properties and application of Turing patterns with the use of deterministic approach is presented. Then we proceed to the stochastic approaches, which allows us to observe special phenomena in the Turing patterns formation, which can not be captured by the deterministic models. In Chapter 4, we introduce the compartment-based SSA. The molecular-base SSA is presented in Chapter 5.

2. Deterministic and stochastic models of well-stirred chemical systems

In this chapter, we introduce a chemical system which is used in this dissertation to illustrate our results. We will use it to explain deterministic and stochastic approaches to modelling reaction-diffusion processes.

2.1 Illustrative Model

We will consider a system of three chemical species A, B and C which are subjects to the following chemical reactions

$$A + A \underset{k_2}{\overset{k_1}{\rightleftarrows}} B \tag{2.1}$$

$$B + C \xrightarrow{k_3} B + A \tag{2.2}$$

$$\emptyset \xrightarrow{k_4} A \tag{2.3}$$

$$A \xrightarrow{k_5} \emptyset \tag{2.4}$$

$$\emptyset \xrightarrow{k_6} C, \tag{2.5}$$

where k_i, $i = 1, 2, \ldots, 6$, are positive reaction rate constants. Presented chemical reactions can be interpreted as follows. The first chemical reaction is reversible dimerisation. It simply means that two molecules of A can react to produce one molecule of B but also one molecule of B can dissociate to produce two molecules of A. Therefore the reaction (2.1) effectively describes two reactions, the forward reaction

$$A + A \xrightarrow{k_1} B \tag{2.6}$$

and backward reaction

$$B \xrightarrow{k_2} A + A. \tag{2.7}$$

The reaction (2.2) describes catalysed izomerisation, i.e change of one molecule to another with the use of a catalyzator. Most enzymatic[1] reactions occurs at

[1]Enzymes are proteins that catalyse chemical reactions. In enzymatic reactions, the molecules at the beginning of the process are called substrates, and they are converted into different molecules, called the products. Almost all processes in a biological cell need enzymes to occur at significant rates.

this manner.
The reactions (2.3) and (2.5) represent a production of molecules of A and C, respectively. The symbol $\emptyset$ denotes chemical species which are of no further interest and which do not react with chemicals A, B and C.
Finally, the reaction (2.4) describes degradation of A molecules. Molecules can not just disappear from the system, but they can convert to molecules of other type which are out of our interest, therefore we denote them as $\emptyset$.

2.2 Deterministic Simulation of Chemical Reactions

In the deterministic approach for the simulation of chemical reactions, we describe each chemical species by its concentration. In particular, we will denote the concentrations of chemical species by corresponding lower-case letters

$$a = [A], \quad b = [B], \quad c = [C],$$

where the symbol [ ] traditionally denote concentration [1]. Then applying the *Law of Mass Action*, which says that the rate of a reaction is proportional to the product of the concentrations of the reactants, to the system $(2.1) - (2.5)$ we obtain a system of ordinary differential equations (ODEs):

$$\begin{aligned} \frac{\mathrm{d}\,a}{\mathrm{d}\,t} &= -k_1 a^2 + k_2 b + k_3 bc + k_4 - k_5 a\,, \\ \frac{\mathrm{d}\,b}{\mathrm{d}\,t} &= k_1 a^2 - k_2 b\,, \\ \frac{\mathrm{d}\,c}{\mathrm{d}\,t} &= -k_3 bc + k_6. \end{aligned} \tag{2.8}$$

To complete the mathematical formulation we endow the system (2.8) with initial conditions

$$a(0) = a_0, \quad b(0) = b_0, \quad c(0) = c_0. \tag{2.9}$$

The solution of the system (2.8) - (2.9) describes the concentration of chemical species as a function of time. As in any reaction kinetics problem we are only concerned with non-negative concentrations. The solution of (2.8) - (2.9) is plotted in the Figure 2.1 as a dash line. More precisely, for the reason of a comparison of the deterministic and the stochastic approach, we plot numbers of molecules of chemical species A, B and C, within some fixed volume ν with concentrations $a(t)$, $b(t)$ and $c(t)$, respectively, defined as

$$\bar{A}(t) = a(t)\nu, \quad \bar{B}(t) = b(t)\nu, \quad \bar{C}(t) = c(t)\nu.$$

Multiplying (2.8) - (2.9) by volume ν, we obtain that the time evolution of $\bar{A}(t)$, $\bar{B}(t)$ and $\bar{C}(t)$ is governed by the system of ODEs:

$$\begin{aligned} \frac{\mathrm{d}\,\bar{A}}{\mathrm{d}\,t} &= -\frac{k_1\bar{A}^2}{\nu} + k_2\bar{B} + \frac{k_3\bar{B}\bar{C}}{\nu} + k_4\nu - k_5\bar{A} \\ \frac{\mathrm{d}\,\bar{B}}{\mathrm{d}\,t} &= \frac{k_1\bar{A}^2}{\nu} - k_2\bar{B} \\ \frac{\mathrm{d}\,\bar{C}}{\mathrm{d}\,t} &= -\frac{k_3\bar{B}\bar{C}}{\nu} + k_6\nu. \end{aligned} \tag{2.10}$$

with initial conditions

$$\bar{A}(0) = a_0\nu, \quad \bar{B}(0) = b_0\nu, \quad \bar{C}(0) = c_0\nu. \tag{2.11}$$

The solution of (2.10) − (2.11) with initial conditions $\bar{A}(0) = 20$, $\bar{B}(0) = 40$ and $\bar{C}(0) = 4$ is plotted as a dash line in Figure 2.1 presented at the end of this chapter.

Remark. (Rescaling of reaction rates)
Comparing the equations (2.8) and (2.10) we see that both of them are represented by the same system of ODEs, but the reaction rates are different. For instance the reaction rate k_1 in (2.8) corresponds to the reaction rate k_1/ν in (2.11). This will be very important in Chapter 4 and 5.

2.3 Stochastic Simulation of Well-Stirred Systems

In stochastic simulations we characterise each chemical species by the number of molecules. Let us consider a system of $N \geq 1$ chemical species A_i, $i = 1, \ldots, N$, which react through $M \geq 1$ chemical reactions R_j, $j = 1, \ldots, M$. We denote by $A_i(t)$ the number of molecules of chemical species A_i at time t. Then the state of the system at a given time t is specified by a vector of states

$$\mathbf{x} \equiv \mathbf{x}(t) = [A_1(t), \ldots, A_N(t)].$$

For example, for the illustrative model (2.1)−(2.5), we have $\mathbf{x}(t) = [A(t), B(t), C(t)]$. To simulate the system of chemical reactions, we would like to describe the evolution of $\mathbf{x}(t)$ from some given initial state $\mathbf{x}_0$. The state of the system is modified by chemical reactions, so we assign to each chemical reaction R_j a vector $\mathbf{v}_j \in \mathbb{R}^N$ whose i-th component $\mathbf{v}_{ji}$ describes a change in number of molecules A_i caused by one reaction R_j. For example, for the reaction (2.6) we have

$$\mathbf{v}_1 = [-2, 1, 0].$$

Since the vector of states is a jump-type Markov process on the non-negative N-dimensional integer lattice, we would like to derive a time evolution equation for the conditional probability $\mathbb{P}(\mathbf{x}, t\,|\mathbf{x}_0, t_0)$, i.e. the probability that the system is in the state $\mathbf{x}$ at time t given that it was in state $\mathbf{x}_0$ at time t_0. Such an equation is called a *Chemical Master equation*.

2.3.1 Chemical Master Equation

As we already know, in a stochastic approach, the system is characterised by number of molecules. From a molecular point of view, we can intuitively accept that chemical reactions involving two or more reactants occur when reacting molecules collide. If we assume the system is well-stirred in some fixed volume with constant temperature, then every pair of reacting molecules have the same probability to react in the infinitesimal small time interval $[t, t + \mathrm{d}\,t)$.
Under these assumption it can be shown that for each chemical reaction, R_j, there will exist a well-defined function α_j called a propensity function [8].

Definition 1. (Propensity function)
Let us consider that the state of the system at time t is given by the vector $\mathbf{x}(t)$. Then the *propensity function* $\alpha_j(\mathbf{x}(t))$ of chemical reaction R_j is defined as a such function that the probability of occurrence of one reaction R_j in the next infinitesimal time interval $[t, t + \mathrm{d}\,t)$ is equal to $\alpha_j(\mathbf{x}(t))\,\mathrm{d}\,t$.

For instance, the propensity function of the chemical reaction (2.2), in the system with some fixed volume ν is defined as

$$\alpha = B(t)C(t)k_2/\nu. \tag{2.12}$$

To derive the formulae (2.12) we can proceed as follows. We assume the system is well-stirred, i.e. each pair of molecules B and C have the same probability to react in the time interval $[t, t + \mathrm{d}\,t)$. This probability is equal to $k_2 dt/\nu$. The number of all pairs of molecules B and C is equal to the product $B(t)C(t)$. Thus the probability that one reaction (2.2) occurs in time interval $[t, t + \mathrm{d}\,t)$ is equal to $B(t)C(t)k_2\,\mathrm{d}\,t/\nu = \alpha(\mathbf{x}(t))\,\mathrm{d}\,t$. In Table 2.1 we present the propensity functions of the chemical reactions from the illustrative model (2.1) − (2.5).
To derive a general form of chemical master equation, let us consider a well-stirred thermally equilibrated chemical system consisting of $N \geq 1$ chemical species A_i, $i = 1, \ldots, N$, which react through $M \geq 1$ chemical reactions R_j, $j = 1, \ldots, M$ inside of some volume ν. To describe the evolution of probability $\mathbb{P}$ we choose a time step $\mathrm{d}\,t$ so small that the probability that two or more reactions occur in time interval $[t, t + \mathrm{d}\,t)$ is negligible compared to the probability that only one reaction takes place. Then we can write the probability of the system being in state $\mathbf{x}$ at time $t + \mathrm{d}\,t$ as a sum of the probabilities of all mutually exclusive

Table 2.1: *The propensity functions of chemical reactions from the illustrative model.*

chemical reaction	propensity function α
$\emptyset \xrightarrow{k} A$	$k\nu$
$A \xrightarrow{k} \emptyset$	$A(t)k$
$B + C \xrightarrow{k} B + A$	$B(t)C(t)k/\nu$
$A + A \xrightarrow{k} B$	$A(t)\,(A(t)-1)\,k/\nu$

ways in which that can happen via either zero or one reaction in time interval $[t, t + \mathrm{d}\,t)$:

$$\begin{aligned}\mathbb{P}\,(\mathbf{x},\, t+\mathrm{d}\,t\,|\mathbf{x}_0,\, t_0) &= \mathbb{P}\,(\mathbf{x},\, t\,|\mathbf{x}_0,\, t_0)\,\left[1-\sum_{j=1}^{M}\alpha_j(\mathbf{x}(t))\;\mathrm{d}\,t\right]\\ &+ \sum_{j=1}^{M}\left[\mathbb{P}(\mathbf{x}-\mathbf{v}_j,\, t\,|\,\mathbf{x}_0,\, t_0)\alpha_j(\mathbf{x}(t))\;\mathrm{d}\,t\right].\end{aligned}$$

After a few simple algebraic rearrangements and by passing the limit $\mathrm{d}\,t \to 0$ we obtain the so-called *Chemical master equation*

$$\begin{aligned}\frac{\partial}{\partial t}\mathbb{P}(\mathbf{x},\, t\,|\mathbf{x}_0,\, t_0) &= \sum_{j=1}^{M}\left[\alpha_j\mathbf{x}(t)\,\mathbb{P}(\mathbf{x}-\mathbf{v}_j, t\,|\mathbf{x}_0,\, t_0)\right.\\ &- \left.\alpha_j\mathbf{x}(t)\mathbb{P}(\mathbf{x},\, t\,|\mathbf{x}_0,\, t_0)\right].\end{aligned} \tag{2.13}$$

For example, if we consider the illustrative model (2.1) − (2.5) is in the state $\mathbf{x} = [A, B, C]$ within fixed volume ν, then the chemical master equation is

$$\begin{aligned}\frac{\partial P(A,B,C)}{\partial t} &= P(A+2,B-1,C)\Big[(A+2)(A-1)k_1/\nu\Big]\\ &+ P(A-2,B+1,C)\Big[(B+1)k_2\Big]\\ &+ P(A-1,B,C+1)\Big[B(C+1)k_3/\nu\Big]\\ &+ P(A-1,B,C)\Big[k_4\nu\Big] + P(A+1,B,C)\Big[(A+1)k_5\Big]\\ &+ P(A,B,C-1)\Big[k_6\nu\Big]\\ &- P(A,B,C)\Big[A(A-1)k_1/\nu + Bk_2 + BCk_3/\nu + k_4\nu + Ak_5 + k_6\nu\Big],\end{aligned}$$

where $P(A, B, C) \equiv \mathbb{P}(A, B, C, t|A_0, B_0, C_0, t_0)$.

In principle, we obtain all the information about the system by solving the chemical master equation. But the exact analytical solution can rarely be obtained in

practice, therefore we turn our efforts to computer - oriented numerical method. In the following section we present a numerical method proposed by D. Gillespie in 1976 [25].

2.3.2 Gillespie Algorithm

Although the chemical master equation provides the exact description of the time evolution of the system, it can only be solved in simple cases. If the system involves more then a few chemical species and chemical reactions the mere formulation of the chemical master equation is impractical. Therefore we introduce a simulation method, called the Gillespie algorithm [25], which is equivalent to solving the master equation, however this equation itself is never explicitly used. The Gillespie algorithm is a simple computational method which does not try to solve the master equation numerically, but instead it numerically simulate the same Markov process that master equation describes analytically.
This algorithm can be explain as follows. Let us consider a well-stirred thermally equilibrated system of $N \geq 1$ chemical species A_i, $i = 1, \ldots, N$, in some fixed volume ν, which are subject to $M \geq 1$ chemical reactions R_j, $j = 1, \ldots, M$. For each reaction R_j we denote the corresponding propensity function as α_j, $j = 1, \ldots, M$, i.e. for simplicity we would omit the dependence of propensity function on the state of the system.
Then at every given time, we ask two questions: At what time does the next reaction occur? And which reaction is it? To answer these questions we define the *reaction probability density function* $P(\tau, j)$ such that

$$P(\tau, j)\,\mathrm{d}\,\tau \equiv \text{ the probability at a time } t \text{ that the } \textit{next} \text{ reaction will occur during the time interval } [t+\tau, t+\tau+\mathrm{d}\,\tau) \textit{ and} \text{ it will be an } R_j \text{ reaction.}$$

It means that $P(\tau, j)$ is a joint probability function on the space of the continuous variable $\tau \in [0, \infty)$ and the discrete variable $j \in \{1, 2, \ldots, M\}$. Let us denote $P_0(\tau)$ the probability at time t that *no* reaction will occur in the time interval $[t, t+\tau)$. Then $P(\tau, j)$ can be computed as a product of $P_0(\tau)$ and the probability that one reaction R_j will occur in interval $[t+\tau, t+\tau+\mathrm{d}\,\tau)$:

$$P(\tau, j)\,\mathrm{d}\,\tau = P_0(\tau)\alpha_j\,\mathrm{d}\,\tau. \tag{2.14}$$

To compute $P_0(\tau)$, imagine the interval $[t, t+\tau)$ is divided into K subintervals, each of length $\varepsilon = \tau/K$. Then using the definition of the propensity function we obtain the probability that no reaction $R_1, \ldots, R_M$ takes place in $[t, t+\varepsilon)$. This probability is

$$1 - \sum_{k=1}^{M} \alpha_k \varepsilon + o(\varepsilon).$$

This is also the *subsequent* probability that no reaction occurs in $[t+\varepsilon, t+2\varepsilon)$ and *then* in $[t+2\varepsilon, t+3\varepsilon)$ and so on. Therefore $P_0(\tau)$ can be written as

$$\begin{aligned} P_0(\tau) &= \left[1 - \sum_{k=1}^{M} \alpha_k \varepsilon + o(\varepsilon)\right]^K \\ &= \left[1 - \sum_{k=1}^{M} \alpha_k \tau/K + o(1/K)\right]^K . \end{aligned}$$

This is true for any $K > 1$, and in particular it is true for $K \to \infty$, therefore we can write

$$P_0(\tau) = \lim_{K\to\infty} \left[1 - \left(\sum_{k=1}^{M} \alpha_k \tau + o(1/K)K^{-1}\right)/K\right]^K .$$

Then using the standard limit formula for the exponential function we obtain

$$P_0(\tau) = \exp\left[-\sum_{k=1}^{M} \alpha_k \tau\right]. \tag{2.15}$$

Remark. It may seem that the easier way of deriving the formula (2.15), is to multiply M individual probabilities $\exp(-\alpha_k\tau)$, corresponding to non-occurrence of each chemical reaction R_k in the time interval $[t, t+\tau)$. However this is not a correct approach, because $\exp(-\alpha_k\tau)$ is the probability that the reaction R_k will not occur in $[t, t+\tau)$ *only* in the absence of all other reactions involving R_k reactants.

If we denote the sum of all propensity functions as

$$\alpha_0 = \sum_{k=1}^{M} \alpha_k .$$

then the reaction probability density function can be expressed as

$$P(\tau, j) = \alpha_j \exp[-\alpha_0 \tau], \tag{2.16}$$

for $0 \le \tau < \infty$ and $1 \le j < M$. For all other values τ and j, $P(\tau, j)$ is zero. Our goal is to find τ such that if the system is in time t, then $t+\tau$ is the time when the next reaction takes place. If we denote $P_1(\tau)$ the sum of $P(\tau, j)$ over all j-values

$$P_1(\tau) = \sum_{j=1}^{M} P(\tau, j), \tag{2.17}$$

then $P_1(\tau)\,\mathrm{d}\,\tau$ is the probability at the time t that the next reaction will occur during the time interval $[t+\tau, t+\tau+\mathrm{d}\,\tau)$ irrespectively of which reaction it might be. Substituting (2.16) into (2.17) we obtain

$$P_1(\tau) = \begin{cases} \alpha_0 \exp(-\alpha_0\tau) & \text{for } 0 \le \tau < \infty, \\ 0 & \text{otherwise.} \end{cases}$$

Then the corresponding probability distribution function is

$$F(\tau) = \exp[-\alpha_0 \tau]. \tag{2.18}$$

Since $\tau \in [0, \infty)$ is a random number distributed according to probability density function $P_1(\tau)$, then $F(\tau)$ is a random number uniformly distributed in the interval $(0, 1)$. To find τ we can generate a random number, denote r_1, uniformly distributed in the unit interval. Then putting $F(\tau) = r_1$ and solving (2.18) for τ we obtain that

$$\tau = \frac{1}{\alpha_0} \ln \left[\frac{1}{r_1} \right], \tag{2.19}$$

where we replace the random variable $1 - r_1$ by the statistically equivalent random variable r_1 for simplicity.

Now when we know the time when the next reaction occurs, we would like to know which one it is. Since the reactions partition the interval $(0, 1)$ according to the size of their propensity functions, we can decide which reaction has occurred at time $t + \tau$ by generating second random number r_2, uniformly distributed in $(0, 1)$, and deciding in which partition r_2 lies. So we say R_j is the reaction that occur in $t + \tau$, if j is the integer for which [7, 54]

$$r_2 \geq \frac{1}{\alpha_0} \sum_{k=1}^{j-1} \alpha_k \quad \text{and} \quad r_2 < \frac{1}{\alpha_0} \sum_{k=1}^{j} \alpha_k. \tag{2.20}$$

Thus the Gillespie algorithm may be outlined as follows:

THE GILLESPIE ALGORITHM

1. Initialisation: set time $t = 0$, specify the initial number of molecules of each chemical species and define a stopping time t_{STOP}.

2. Generate two random numbers r_1 and r_2 uniformly distributed in $(0, 1)$.

3. For each chemical reaction compute the propensity function α_i, $i = 1, \ldots, M$. Compute the sum of all propensity functions

$$\alpha_0 = \sum_{k=1}^{M} \alpha_k.$$

4. Compute the time when the next chemical reaction occurs as $t + \tau$ where

$$\tau = \frac{1}{\alpha_0} \ln \left[\frac{1}{r_1} \right]$$

5. Use the random number r_2 to decide which reaction takes place at time $t+\tau$. It means, find such j that the condition (2.20) holds.

6. Let the reaction R_j occurs, i.e. update the number of molecules of those chemical species which involved in reaction R_j.

7. Set $t = t + \tau$ and continue with the step 2 until $t > t_{STOP}$.

One realisation of the Gillespie algorithm corresponds to a random evolution of the system governed by the chemical master equation. Thus, by repeating the execution of the algorithm, starting from the same initial state and proceeding to the same time t, an average that corresponds to the solution of the master equation will be obtained.

Let us consider the illustrative model $(2.1) - (2.5)$ in the domain with volume $\nu = 10\ \mu m^3$ and initial state given by $A(0) = 20$, $B(0) = 40$ and $C(0) = 4$. We choose the rate constants as follows: $k_1 = 1\ \mu m^3 sec^{-1}$, $k_2 = 1\ sec^{-1}$, $k_3 = 2\ \mu m^3 sec^{-1}$,

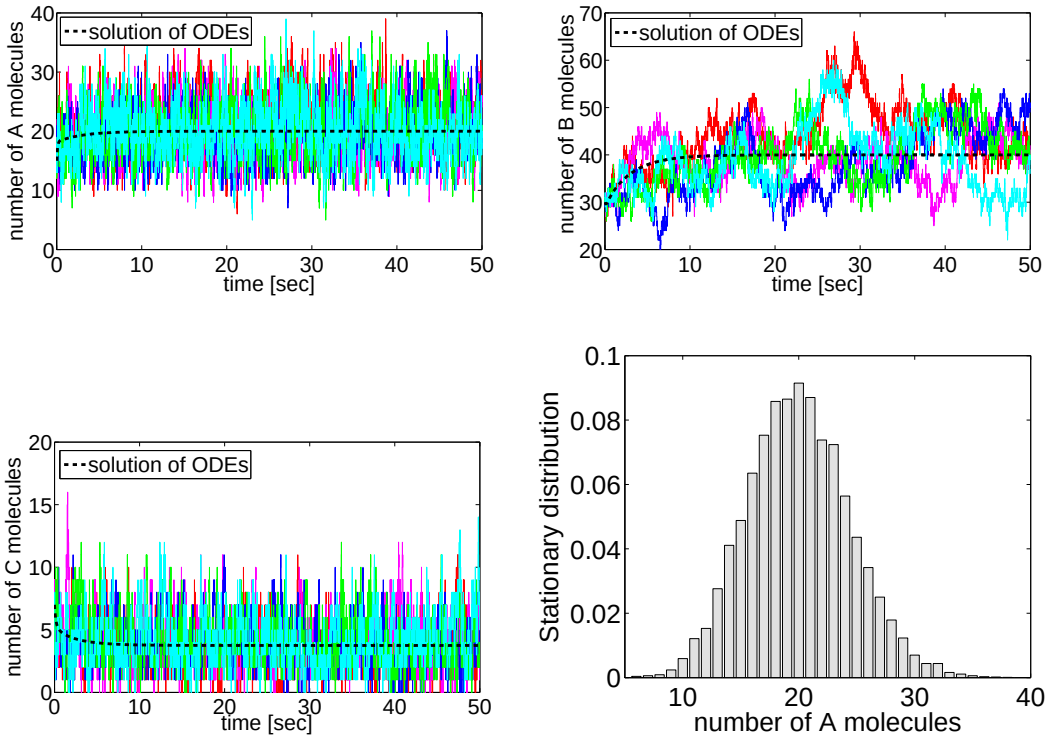

Figure 2.1: *Stochastic simulation of the system of chemical reactions* $(2.1)-(2.5)$ *for* $A(0)=20$, $B(0)=40$, $C(0)=4$ *and for reactions rates specified above. On the first three figures we plot* $A(t)$, $B(t)$ *and* $C(t)$ *respectively, given by five realisations of the Gillespie algorithm, as solid lines. Each color corresponds to one realisation. The solution of the system of ODEs* $(2.10)-(2.11)$ *is plotted in the same figures as the dash line. In the last figure we plot the stationary distribution of molecules of* A*, obtained by long time simulations of the Gillespie algorithm.*

$k_4 = 1\ \mu m^{-3} sec^{-1}$, $k_5 = 2\ sec^{-1}$ and $k_6 = 3\ \mu m^{-3} sec^{-1}$. In the figure 2.1 we present five realisations of the Gillespie algorithm of this model. We plot number of molecules as a functions of time as a solid lines. In the same figure we plot the deterministic solution of $(2.10)-(2.11)$ as a dashed line. We can see that the stochastic solution fluctuates around the deterministic one.

Remark. The Gillespie algorithm is a simple and efficient method for simulation of chemical reactions, but it may become computationally intensive if we consider a system with large numbers of chemical reactions. In such case we can increase its efficiency as follows. At the beginning of the simulation we compute the propensity functions of all reactions. We assume that in one time step only one reaction takes place, therefore in the third step of the algorithm it is enough to compute only those propensity functions which are changed by a reaction selected in previous time step [7].

Remark. Both presented stochastic approaches, chemical master equation and Gillespie algorithm, are based on the assumption that the system is well-stirred. If this is not true then the stochastic formulation of chemical kinetics would not be valid. However in such a situation we can not expect that the usual deterministic formulation would be valid either, because it presupposes uniform concentrations for all chemical species. In this case we need to consider a molecular-based approach where the positions and the velocities of all the molecules are accounted. This approach is presented in Chapter 5.

3. Spatial Pattern Formation with Reaction Diffusion Systems

3.1 Role of Turing Patterns in Biology

In 1952, Alan Turing suggested that under certain conditions, chemicals can react and diffuse in such way as to produce spatial patterns of chemical or morphogen[1] concentration. This assumption plays an important role in developmental biology and embryology. Here pattern formation is used to describe mechanisms by which initially homogeneous tissue develop in a spatially and functionally differentiated structures. Despite the ubiquity of the patterns it is still unknown how they are laid down. Therefore an understanding of the pattern formation is without question one of the major fundamental scientific challenges.
In recent years considerable progress has been made on several different fronts. For instance, formation mechanisms in limb bud development [20], pigmentation patterning in mammalian coats [1] or formation of skin follicules of mice [12] have been explained. Nowadays the role of pattern mechanisms in the development of a model for the regulatory network that governs lung or ureteric duct branching [19] is studied.
In this chapter we will study the mechanism responsible for pattern formation. More precisely, we will consider the illustrative three-component system for which we derive necessary and sufficient conditions under which patterns are laid down. We present these conditions in a greater generality.

3.2 Reaction Diffusion (Turing) Mechanisms

Let us consider a general reaction-diffusion system of $n \geq 1$ components. We denote by $\mathbf{u} = (u_1, u_2, \ldots, u_n)$ a vector of concentrations of chemical species. Then the reaction diffusion mechanisms of this system is described by n reaction-diffusion equations:

$$\frac{\partial u_j}{\partial t} = D_j \Delta u_j + f_j(\mathbf{u}) \tag{3.1}$$

$j = 1, \ldots, n$, defined in the time-space cylinder $Q_T = \Omega \times (0, T)$, where $T > 0$ and $\Omega \subset \mathbb{R}^N$, $(N = 1, 2, 3)$ is a bounded domain. Here Δ denotes the Laplace

[1] A morphogen is a substance that induces different cell fates in a concentration dependent manner. It is especially important in development because emission of a morphogen from a source can lead to the formation of different cell types in a defined spatial relationship to the source and to each other.

operator, D_j is the diffusion coefficient of the j-th species and f_j is a reaction term, i.e the term which takes into account chemical reactions which modify the concentration of the species u_j. To complete the system we equip equation (3.54) with initial conditions

$$u_j(\mathbf{x}, 0) = u_{j0}(\mathbf{x}), \quad j = 1, \ldots, N \tag{3.2}$$

and boundary conditions:

$$\mathbf{n} \cdot \nabla u_j \mid_{\partial\Omega\times(0,T)} = 0, \quad j = 1, \ldots, N \tag{3.3}$$

where $\mathbf{n}$ is the unit outward normal to $\partial\Omega$. A reason why we consider the zero flux boundary conditions is that we are interested in self-organisation of patterns and the zero flux conditions imply no external input. Then we can define patterns as follows.

Definition 2. [11] *Patterns* are stable, time-independent, spatially heterogeneous solutions of the system of equations (3.54)-(3.3).

We say that the reaction-diffusion system produces Turing patterns if it fulfils the condition of diffusion-driven instability, also referred as Turing instability.

Definition 3. A *diffusion-driven instability* occurs when a homogeneous steady state, stable to small spatial perturbation in the absence of diffusion goes unstable when diffusion is present.

This conditions may be a bit surprising because diffusion is usually considered as a stabilising process. To see intuitively how diffusion can be destabilising consider following, a bit unrealistic, but illustrative example presented in [1].

Example. Let us consider a field of dry grass where a large number of grasshoppers live. They have the ability to produce moisture by sweating when they get warm. Now suppose that we set a fire at some point and that the flame front starts to spread. This should be described as a system of two chemical species, the fire, which acts as an activator, and the grasshoppers, which behave as an inhibitor. If there is no moisture in the system, then the fire would spread over the whole field and would result in a uniform charred area.
However if we assume that grasshoppers can produce enough moisture to dampen the grass so that when the fire reaches such pre-moistened area the grass will not burn, we can describe pattern formation as follows. We know that the fire spread in the domain, so we can assume that it diffuses with some diffusion coefficient denote D_F. When the grasshoppers ahead of the flame front feel it is coming they move quickly ahead of it, it means they diffuse with some diffusion coefficient D_G. We will assume that D_G is larger than D_F, otherwise the grasshoppers

do not have a chance to survive, and we again obtain a uniform charred area. When the grasshoppers run away, they sweat and so produce enough moisture to prevent the fire spreading into the moistened area. In this way the charred area is restricted to a finite domain which depends on the diffusion coefficients of reactants and other reaction parameters.
If, instead of a single initial fire, there wes a random scattering of them, then this process would result in a final spatially heterogeneous steady state distribution of charred and uncharred areas in the field and a spatial distribution of grasshoppers, since the above scenario takes place around each fire. If both reactants diffused at the same speed, no such pattern formation could occur. Therefore one of the necessary conditions for existence of Turing patterns is that at least one of the diffusion coefficients must be different.

Before we proceed to the derivation of the necessary and sufficient conditions under which Turing instability will arise, let us summarise some useful statements and notations.
Consider a square $(n \times n)$ matrix A. Let $1 \leq i_1 < i_2 < \cdots < i_p \leq n$, $(1 \leq p \leq n)$ be distinct indices from the set $1, 2, \ldots, n$. We denote by $A_{i_1 i_2 \ldots i_p}$ the square submatrix obtain from A by taking exactly the rows and the columns of indices i_1, $i_2, \ldots, i_p$ and its determinant would be denoted by $\triangle_{i_1, i_2, \ldots, i_p}$. To derive the conditions for the Turing instability, it is useful to know the Routh-Hurwitz criterion, which provides necessary and sufficient stability conditions.

Theorem 1. *(Routh-Hurwitz criterion)*
Let A be a square $(n \times n)$ matrix with a characteristic polynomial

$$P(\lambda) \;\; = \;\; \lambda^n + a_1 \lambda^{n-1} + \cdots + a_{n-1}\lambda + a_n,$$

where the coefficients a_i are real constants, $i = 1, \ldots, n$ given by:

$$a_1 = -\sum_{1 \leq i \leq n} \triangle_i \,; \quad a_2 = \sum_{\substack{1 \leq i,j \leq n \\ i<j}} \triangle_{i\,j} \,; \quad \ldots \,; \quad a_n = (-1)^n \triangle_{1,2,\ldots,n} \,. \tag{3.4}$$

Using these coefficients we define n Hurwitz matrices as follows:

$$H_1 = (a_1), \quad H_2 = \begin{pmatrix} a_1 & 1 \\ a_3 & a_2 \end{pmatrix}, \quad H_3 = \begin{pmatrix} a_1 & 1 & 0 \\ a_3 & a_2 & a_1 \\ a_5 & a_4 & a_3 \end{pmatrix}$$

and

$$H_n = \begin{pmatrix} a_1 & 1 & 0 & 0 & \ldots & 0 \\ a_3 & a_2 & a_1 & 1 & \ldots & 0 \\ a_5 & a_4 & a_3 & a_2 & \ldots & 0 \\ \vdots & \vdots & \vdots & \vdots & \ldots & \vdots \\ 0 & 0 & 0 & 0 & \ldots & a_n \end{pmatrix}$$

where $a_j = 0$ if $j > n$. Then the following statement is true. All of the roots of the polynomial $P(\lambda)$ are negative or have negative real part iff the determinants of all Hurwitz matrices are positive:

$$\det H_j > 0, \quad j = 1, 2, \ldots, n. \tag{3.5}$$

It means we can say a matrix is stable if the conditions set by above criterion are fulfilled. For the proof of the Routh-Hurwitz criterion please see [28].

Remark. For polynomials of degree $n = 2, 3, 4$, the Routh-Hurwitz criteria are

n=2: $a_1 > 0$ and $a_2 > 0$

n=3: $a_1 > 0$, $a_3 > 0$ and $a_1 a_2 > a_3$

n=4: $a_1 > 0$, $a_3 > 0$, $a_4 > 0$ and $a_1 a_2 a_3 > a_3^2 + a_1^2 a_4$.

Definition 4. Let A be a square $(n \times n)$ matrix. We say that A is s-stable if, for any minor $\triangle_{j_1, j_2, \ldots, j_q}$ of order q, $1 \leq q \leq n$, we have

$$\operatorname{sgn}(\triangle_{j_1, j_2, \ldots j_g}) \;=\; (-1)^q. \tag{3.6}$$

This means that the matrix A is s-stable if each of its subsystems is stable.

Theorem 2. *(Descartes Sign Rule)*
Let $p(x) = \sum_{i=0}^{m} a_i x^i$ be a polynomial with real coefficients such that $a_m \neq 0$. Define v to be the number of variations in sign of the sequence of coefficients $a_m, \ldots, a_0$. By "variations in sign" we mean the number of values of n such that the sign of a_n differs from the sign of a_{n-1} , as n ranges from m down to 0. Then the number of positive real roots of $p(x)$ is either equal to v or is less than it by a multiple of 2. Multiple roots of the same value are counted separately.

This means that a polynomial with real coefficients has at most v positive roots. The exclusion of multiples of 2 is because the polynomial may have complex roots which always come in pairs. Since the negative roots of the polynomial equation $p(x) = 0$ are positive roots of the equation $p(-x) = 0$, the rule can be readily applied to help count the negative roots as well. For the proof of the Descartes sign rule please see [31].

Remark. Descartes sign rule can only be used to determine the sign of real roots, it does not hold for the sign of the real part of a complex root. For example, consider polynomial

$$p(x) = x^4 + x^2 - 2x + 6. \tag{3.7}$$

Number of variation in sign of $p(x)$ is two. It means that this polynomial has two or zero positive real roots. On the other hand number of variation in sign

of $p(-x)$ is zero, it means that there are no negative real roots. In this case the Descartes rule implies that the system has two or four complex roots, but it tells nothing about the stability. In this case the polynomial $p(x)$ has four imaginary roots, two with positive real part and two with negative real part.

3.3 Conditions for Diffusion-Driven Instability

The idea of the derivation of Turing instability conditions is quite simple. Let us denote $\mathbf{u}_s$ the homogeneous steady state of $(3.54) - (3.3)$. To prove the Turing instability we first need to show that this solution is linearly stable as the solution of a kinetic system:

$$\frac{\partial u_j}{\partial t} = f_j(\mathbf{u}), \quad u_j(0) = u_{j0} \tag{3.8}$$

for $j = 1, \ldots, n$. To study this we linearise the system (3.8) about the steady state $\mathbf{u}_s$, it means we set $\mathbf{w} = (\mathbf{u} - \mathbf{u}_s)$ and for $|\mathbf{w}|$ small we obtain,

$$\mathbf{w}_t = A\mathbf{w}, \quad \mathbf{n} \cdot \nabla \mathbf{w} = 0, \quad \mathbf{w}(\mathbf{x}, 0) = 0, \tag{3.9}$$

where $A = \{a_{ij}\}_{i,j=1}^{n}$ is the Jacobian matrix associated with (3.8) at $\mathbf{u} = \mathbf{u}_s$, i.e. $a_{ij} = \frac{\partial f_j}{\partial u_j}(\mathbf{u}_s)$, $1 \leq i, j \leq n$. The system (3.9) is linear and so we look for a solution in the form

$$\mathbf{w} \propto \exp(\lambda t),$$

where λ is the eigenvalue of A. The steady state $\mathbf{w} = 0$ is linearly stable if all the eigenvalues of A have negative real parts, because in this case the perturbation $\mathbf{w} \to 0$ as $t \to \infty$.

Once we would know that $\mathbf{u}_s$ is stable solution of (3.8), i.e. it is stable solution of the system $(3.54) - (3.3)$ without diffusion, we have to prove that it becomes unstable when diffusion is present. So let us consider the full reaction-diffusion systems $(3.54) - (3.3)$ and linearise it about the steady state $\mathbf{w} = 0$ to obtain

$$\mathbf{w}_t = A\mathbf{w} + D\Delta\mathbf{w}\,, \quad \mathbf{n} \cdot \nabla \mathbf{w} = 0\,, \quad \mathbf{w}(\mathbf{x}, 0) = 0, \tag{3.10}$$

where D is matrix of diffusion constants defined as $d_{ij} = D_i\delta_{ij}$, where δ_{ij} is the Kronecker delta. To solve this system of equations we first define $\mathbf{W}(\mathbf{x})$ to be time-independent solution of a spatial eigenvalue problem defined by

$$\Delta\mathbf{W} + k^2\mathbf{W} = 0 \quad \text{in} \quad \Omega, \tag{3.11}$$

$$(\mathbf{n} \cdot \nabla)\,\mathbf{W} = 0 \quad \text{on} \quad \partial\Omega, \tag{3.12}$$

where $k \in \mathbb{R}$ is the eigenvalue of the above eigenvalue problem. Since Ω is bounded domain in $\mathbb{R}^N$ the eigenfunctions of the Laplace operator form orthonormal basis

in the Hilbert space $L^2(\Omega)$.
For example if $\Omega = [0, a]$, then the solution of the eigenvalue problem (3.11) − (3.12) is $\mathbf{W} \propto \cos(n\pi x/a)$, where $n \in \mathbb{Z}$. In this case, the eigenvalue is $k = n\pi/a$. So, $1/k = a/n\pi$ is a measure of the wavelike pattern and $\omega = 2\pi/k = 2a/n$ is the wavelength in this example.
Since the system (3.10) is a linear problem, we look for its solutions $\mathbf{w}(\mathbf{x}, t)$ in the form

$$\mathbf{w}(\mathbf{x}, t) = \sum_k b_k e^{\lambda t} \mathbf{W}_k(\mathbf{x}) \,, \tag{3.13}$$

where $\mathbf{W}_k(\mathbf{x})$ is the solution of eigenvalue problem (3.11) − (3.12) corresponding to the eigenvalue k. The constants b_k are determined by a Fourier expansion of the initial conditions in terms of $\mathbf{W}_k(\mathbf{x})$ and λ is the eigenvalue which determines temporal growth. Substituting the form (3.13) into (3.10), using (3.11) − (3.12) and cancelling $e^{\lambda t}$, we get for each k:

$$\begin{aligned} \lambda \mathbf{W}_k &= A\mathbf{W}_k + D\Delta \mathbf{W}_k \\ &= A\mathbf{W}_k - D\, k^2 \mathbf{W}_k. \end{aligned}$$

It means the eigenvalues of the system (3.10) are also eigenvalues of the system

$$\mathbf{w}_t = C\mathbf{w} \,, \quad \mathbf{n} \cdot \nabla \mathbf{w} = 0 \,, \quad \mathbf{w}(\mathbf{x}, 0) = 0, \tag{3.14}$$

where

$$C = A - Dk^2. \tag{3.15}$$

Therefore to prove the instability of the system (3.10) it is sufficient to show instability of the simpler system (3.14).
Now we can finally derive the conditions for the Turing instability. The following two theorems together provide necessary and sufficient conditions, set on the matrix A, under which the Turing instability arise. In both of these theorems we would follow the approach presented by Satnoianu at. all in [29].

Theorem 3. *If the kinetic system* (3.9) *of the problem* (3.54) − (3.3) *is s-stable then no Turing bifurcation is possible from the uniform steady state solution* $\boldsymbol{u}_s$ *for any* $n \geq 1$.

Proof. We prove this theorem by induction on n. At first we show that if $n = 1$ then no Turing bifurcation is possible. Indeed, if $n = 1$ we have a single reaction-diffusion equation of the form

$$\frac{\partial u}{\partial t} = D\Delta u + f(u). \tag{3.16}$$

Here $u = u_1$ and $D = D_1$. Let us denote by S the set $\{u_s > 0 \mid f(u_s) = 0\}$ of all homogeneous stable steady states of (3.16). Since u_s from this set are stable, we have

$$f'(u_s) < 0 \tag{3.17}$$

for all $u_s \in S$. Now studying the stability of elements in the set S to the full reaction-diffusion system (3.16), we find that the eigenvalues are given by

$$\lambda = -k^2 + f'(u_s). \tag{3.18}$$

From (3.18) it is clear that $Re(\lambda) < 0$ for all real k. Therefore no Turing instability is possible in this case.

So our induction hypothesis is this: we take a system of n interacting species such that every $(n-1)$ dimensional subsystem is s-stable. We want to show that then the whole system is s-stable. To do this, we need to show that the matrix C defined by (3.15) is s-stable.

At first let us note that it is sufficient to prove this when only one of the diffusion coefficients D_i is non-zero, we choose it to be D_1. See the remark following the proof to see how this can be used to prove the general case with non-zero coefficients. So we need to show that if A is s-stable then the matrix $C = A - dB$ is s-stable, too. Here $d = k^2 D_1 > 0$ and B is $(n \times n)$ matrix, such that $b_{ij} = \delta_{1,1}$.

Let us denote by $\lambda_1, \lambda_2, \ldots, \lambda_n$ the eigenvalues of matrix C. Then its characteristic polynomial is of the form

$$P_n(\lambda) \;=\; \lambda^n + c_1\lambda^{n-1} + \cdots + c_{n-1}\lambda + c_n, \tag{3.19}$$

where coefficients c_i are given by:

$$\begin{aligned}
c_1 &= d - \sum_{i=1}^{n} \triangle_i = d + a_1 \\
c_2 &= -d \sum_{i=2}^{n} \triangle_i + \sum_{1 \le i < j \le n} \triangle_{ij} = -d \sum_{i=2}^{n} + a_2 \\
&\vdots \\
c_n &= d(-1)^{n-1} \triangle_{2\ldots n} + (-1)^n \triangle_{12\ldots n} = d(-1)^{n-1} \triangle_{2\ldots n} + a_n,
\end{aligned} \tag{3.20}$$

where a_i, $i = 1, 2 \ldots n$, are coefficients of the characteristic polynomial associated to the kinetic matrix A defined in (3.4). We assume that A is s-stable, i.e.

$$\triangle_i < 0\,, \quad \triangle_{ij} > 0 \quad , \ldots , \quad \operatorname{sgn}(\triangle_{12\ldots n}) = (-1)^n \tag{3.21}$$

We also assume that $d > 0$. Thus c_i is positive for each $i = 1, \ldots n$. It means that (3.19) is a polynomial of degree n with all coefficients real and positive. Then the

Descartes sign rule implies that all real roots of (3.19) must be negative. However $P(\lambda)$ can also has complex roots. Therefore we will now analyse this possibility. Let us remark that the coefficients c_i defined in (3.20) are differentiable functions of $d > 0$ with the property that

$$c_i(0) = a_i \quad \text{and} \quad c_i(d) > a_i$$

for all $i = 1, \ldots, n$. Taking the derivative (denoted by $'$) of each coefficient in turn with respect to d we have

$$c_1' = 1\,; \quad c_2' = -\sum_{i=2}^{n} \triangle_i\,; \quad \ldots \quad c_n' = (-1)^{n+1} \triangle_{2\,3\ldots(n-1)}. \tag{3.22}$$

From (3.21) we see that all these derivatives are positive.
To decide whether or not the matrix C has eigenvalues with positive real parts we will use the following strategy. Consider C as a matrix with constant coefficients of a linear $n \times n$ system of first order differential equations

$$\frac{\mathrm{d}\,x}{\mathrm{d}\,t} = Cx, \quad \text{for} \quad x \in \mathbb{R}^n,\ t > 0 \quad \text{and} \quad x(0) = x_0.$$

The sign of real parts of the eigenvalues of C dictates the asymptotic behaviour of the solutions. To quantify this behaviour we employ the method of steepest descent. Namely we consider the equation $P(\lambda(x)) = 0$ with the root x taken to be complex. The asymptotic dynamics as $t \to \infty$ may be determined by looking at the saddle points, i.e. points in the complex plain where

$$\frac{\mathrm{d}\,\lambda}{\mathrm{d}\,x} = 0\,.$$

From the equation for the characteristic polynomial we find

$$\lambda' \left[n\lambda^{n-1} + (n-1)c_1\lambda^{n-2} + \ldots + c_{n-1} \right] + c_1'\lambda^{n-1} + c_2'\lambda^{n-2} + \ldots + c_n' = 0\,.$$

Since $\lambda' = 0$, the saddle points satisfy a polynomial equation of degree $(n-1)$ with coefficients c_j', $j = 1, \ldots, n$. It means that there are exactly $n-1$ complex values λ_j such that $\lambda' = 0 \Rightarrow \lambda = \lambda_j$, $j = 1, \ldots, n-1$. Using equations (3.20) and (3.22) we can see that the equation

$$c_1'\lambda^{n-1} + c_2'\lambda^{n-2} + \ldots\, c_n' = 0$$

corresponds exactly to the characteristic polynomial of the system with $n-1$ species which is the subsystem of A with matrix $A_{2\ldots n}$. Then our induction hypothesis implies that

$$Re(\lambda_j) < 0$$

for all $j = 1, \ldots, n-1$. Therefore we deduce that the function $Re(\lambda(d))$ is maximal for $\lambda = \lambda_j$ and therefore for all $d > 0$ we have

$$Re(\lambda) \leq Re(\lambda_j) < 0$$

where $\lambda = \lambda(d)$ is any solution of (3.19). So we have proved that the matrix C is s-stable and therefore there is no Turing bifurcation. □

Remark. The general case where all diffusion coefficients are non-zero may be readily obtained by applying inductively the above proof to each coefficient in turn. Indeed this can be achieved by realising that once A is s-stable than the matrix C is s-stable, too. This may be generalised by considering each entry from the main diagonal iteratively.

We now take matrix C as defined in (3.15), it means we will consider that all the diffusion coefficients are non-zero. Our aim is to show that the condition from Theorem 3 is optimal in the sense that if A is *not* s-stable, than we can tune the diffusion coefficients so that the homogeneous steady state solution $\mathbf{u}_s$ undergoes a Turing bifurcation for the full reaction-diffusion problem (3.54) – (3.3).

Theorem 4. *If the kinetic system* (3.9) *of the problem* (3.54) – (3.3) *is stable and contains an unstable subsystem, then Turing bifurcation is possible from the homogeneous steady state solution* $\boldsymbol{u}_s$.

Proof. As in the previous proof, we define the characteristic polynomial associated to the C by (3.19) where coefficients c_i are now given by

$$\begin{aligned} c_n &= k^{2n} D_1 D_2 \ldots D_n - k^{2n-2} \sum_{\substack{\{i_1,\ldots,i_p\}= \\ \{1,\ldots,n\}-\{i\}}} \triangle_i D_{i_1} D_{i_2} \ldots D_{i_p} + \qquad (3.23) \\ &+ k^{2n-4} \sum_{\substack{\{i_1,\ldots,i_p\}= \\ \{1,\ldots,n\}-\{i,j\} \\ i<j}} \triangle_{ij} D_{i_1} \ldots D_{i_p} - \cdots + (-1)^n \triangle_{12\ldots n} . \end{aligned}$$

Based on the theorem hypothesis we deduce that there are distinct indices $1 \leq i_1 < i_2 < \cdots < i_p \leq n$, $(1 \leq p \leq n)$ taken from the set $1, 2, \ldots, n$ such that the corresponding subsystem is unstable. We also know that $p < n$ because the matrix A is stable by the hypothesis. To prove the existence of Turing bifurcation in this case we show that we can choose the diffusion coefficients in such way that the matrix C has a zero eigenvalue. Obviously this happens if c_n becomes zero for suitably chosen diffusion coefficients D_i, $i = 1, \ldots, n$. To do this we choose a positive, small number ε and let

$$D_{i_1} = D_{i_2} = \cdots = D_{i_p} = \varepsilon .$$

Let $q = n - p$ and denote by the remaining indices from the set $1, 2, \ldots, n$ by $j_1, j_2, \ldots, j_q$. From the equation (3.23) we can see that if all diffusion coefficients, except one (D_{j_1} say) are equal to ε then we have

$$c_n \;=\; (-1)^{n-1} \triangle_J \, D_{j_1} \;+\; (-1)^n \triangle_{12\ldots n} \;+\; O(\varepsilon),$$

where $J = \{1, 2, \ldots, n\} \setminus \{j_1\}$. We can always assume that $\triangle_J$ is non-zero. Otherwise all the minors of order $(n-1)$ would be zero, what would imply that matrix A is a singular matrix. This contradicts the hypothesis that the matrix A has eigenvalues with only negative real parts. Then it is clear that, independent of the sign of $\triangle_J$, we can always find critical value $\delta_c(\varepsilon) > 0$ such that choosing D_{j_1} sufficiently close to $\delta_c(\varepsilon)$ will make c_n take both negative and positive values depending on whether D_{j_1} is less then, or equal to $\delta_c(\varepsilon)$, or greater than $\delta_c(\varepsilon)$. Thus c_n is exactly zero when $D_{j_1} = \delta_c(\varepsilon)$ and thus C has a zero eigenvalue. This means that at $\delta_c(\varepsilon)$ there is a pitchfork bifurcation (with a zero eigenvalue) which corresponds to a Turing bifurcation for the full reaction-diffusion system, and the theorem is proved. □

It means that the Theorem 3 provides the necessary and the Theorem 4 the sufficient condition for the Turing bifurcation to occur in a general n-dimensional reaction-diffusion system. Due to this we can decide whether the given system can produce Turing patterns or not.

3.4 Turing Patterns in the Illustrative Chemical System

In this section we apply our knowledge of pattern formation to the illustrative model introduced in previous chapter. It means we will consider a system of three chemical species A, B and C, which diffuse with diffusion constants D_a, D_b and D_c and react according to (2.1) − (2.5). Then the reaction-diffusion mechanism of this system is governed by following equations

$$\frac{\partial a}{\partial t} \;=\; D_a \Delta a - k_1 a^2 + k_2 b + k_3 bc + k_4 - k_5 a \tag{3.24}$$

$$\frac{\partial b}{\partial t} \;=\; D_b \Delta b + k_1 a^2 - k_2 b \tag{3.25}$$

$$\frac{\partial c}{\partial t} \;=\; D_c \Delta c - k_3 bc + k_6 \tag{3.26}$$

defined in the time-space cylinder $Q_T = \Omega \times (0, T)$, where $T > 0$ and $\Omega \subset \mathbb{R}^N$, $(N = 1, 2, 3)$, is the bounded domain. There the functions a, b and $c : \Omega \times [0, T] \to [0, \infty)$ denote concentration of corresponding chemical species. To complete the system we equip the above equations with the initial conditions

$$a(\mathbf{x}, 0) = a_0(\mathbf{x}), \quad b(\mathbf{x}, 0) = b_0(\mathbf{x}), \quad c(\mathbf{x}, 0) = c_0(\mathbf{x}) \quad \text{for } \mathbf{x} \in \Omega \tag{3.27}$$

and zero-flux boundary conditions

$$\mathbf{n} \cdot \nabla a \mid_{\partial\Omega\times(0,T)} = 0, \quad \mathbf{n} \cdot \nabla b \mid_{\partial\Omega\times(0,T)} = 0, \quad \mathbf{n} \cdot \nabla c \mid_{\partial\Omega\times(0,T)} = 0. \tag{3.28}$$

Then we can use Theorem 3 and Theorem 4 to find necessary and sufficient conditions on the kinetic matrix A, defined in (3.9), under which there exits such diffusion coefficients that the system $(3.24) - (3.28)$ undergoes Turing instability. However these theorems do not specify how to choose the diffusion coefficients. This is the aim of the following theorem, where we derive necessary and sufficient conditions on the whole reaction-diffusion system under which the illustrative mode posses Turing instability.
At first we summarize the notation that would be used. For easier handling we denote the reaction terms from $(3.24) - (3.26)$ as

$$\begin{aligned} f(a,b,c) &= -k_1a^2 + k_2b + k_3bc + k_4 - k_5a \\ g(a,b) &= k_1a^2 - k_2b \\ h(b,c) &= -k_3bc + k_6. \end{aligned}$$

Let us denote by (a_s, b_s, c_s) the homogeneous steady state of $(3.24) - (3.26)$. Since g does not depend on c and h is independent of a, the Jacoby matrix A associated to the system $(3.24) - (3.26)$ is given by

$$\mathbf{A} = \begin{pmatrix} f_a & f_b & f_c \\ g_a & g_b & 0 \\ 0 & h_b & h_c \end{pmatrix}_{(a_s,b_s,c_s)} . \tag{3.29}$$

Here the indices a, b and c of functions f, g and h denote the partial derivative of the function with respect to the corresponding index, for example $f_a := \frac{\partial f}{\partial a}$. From now on we take the partial derivatives of f, g and h to be evaluated at the steady state (a_s, b_s, c_s) unless stated otherwise. The sign of these derivatives would be important in the following theorem, therefore let us summarise it at this place. Since we assume the concentrations and the reaction rates to be non-negative numbers, we obtain that

$$\operatorname{sgn}(A) = \begin{pmatrix} -1 & +1 & +1 \\ +1 & -1 & 0 \\ 0 & -1 & -1 \end{pmatrix}. \tag{3.30}$$

Now we can proceed to the theorem.

Theorem 5. *(Conditions for Turing Instability for the Illustrative system) The Turing instability of the system* $(3.24) - (3.28)$ *occurs if the following conditions hold:*

1) $f_a + g_b + h_c < 0$

2) $f_b\, g_a\, h_c - f_a\, g_b\, h_c - f_c\, g_a\, h_b > 0$

3) $(-f_a - g_b - h_c)\,(f_a\, g_b - f_b\, g_a + f_a\, h_c + g_b\, h_c) > (f_b\, g_a\, h_c - f_a\, g_b\, h_c - f_c\, g_a\, h_b)$

4) $f_a\, g_b - f_b\, g_a < 0$

5) $D_c\, f_a\, g_b + D_a\, g_b\, h_c + D_b\, f_a\, h_c - D_c\, f_b\, g_a \leq 0$

6) And if there exists a time-independent solution $\boldsymbol{W}(\boldsymbol{x})$ *of the eigenvalue problem* (3.11) − (3.12) *with the eigenvalue* k*, within a finite range interval* $[k_1, k_2]$*, such that the polynomial satisfied* $y(k)=Ak^6 + Bk^4 + Ck^2 + D$ *is true that* $y(k_1) = 0$, $y(k_2) = 0$, *and* $y(k) < 0$ *for each* $k \in [k_1, k_2]$*, where*

$$\begin{aligned} A &= D_a\, D_b\, D_c \\ B &= -\, D_a\, D_c\, g_b - D_b\, D_c\, f_a - D_a\, D_b\, h_c \\ C &= \;\; D_c\, f_a\, g_b + D_a\, g_b\, h_c + D_b\, f_a\, h_c - D_c\, f_b\, g_a \\ D &= -\, f_a\, g_b\, h_c - f_c\, g_a\, h_b + f_b\, g_a\, h_c. \end{aligned}$$

Proof. To prove this theorem we have to show that the conditions 1) − 6) are in accordance with conditions required by the definition of Turing instability. **Part 1.** Conditions 1) − 4).
Let us consider the system (3.24) − (3.26) without diffusion, i.e with zero diffusion coefficients. Then after linearising about the steady state (a_s, b_s, c_s) we obtain

$$\mathbf{w}_t = A\mathbf{w}, \quad \mathbf{n} \cdot \nabla \mathbf{w} = 0, \quad \mathbf{w}(\mathbf{x}, 0) = 0,$$

where $\mathbf{w} = (a - a_s, b - b_s, c - c_s)$ and A is the Jacobian matrix given by (3.29). According to Theorem 4, A has to be stable and need to contain an unstable subsystem. The Routh-Hurwitz criteria states that the (3×3) matrix is stable if coefficients a_i, $i = 1, 2, 3$ defined by (3.4), fulfil:

$$a_1 > 0, \quad a_3 > 0, \quad \text{and} \quad a_1\, a_2 > a_3. \tag{3.31}$$

If we compute the coefficients a_i for the matrix A, according to the formulas (3.4), and substitute them in (3.31) we obtain the conditions 1) − 3).
The matrix A contains an unstable subsystem if at least one of the submatrices: A_i, $i = 1, 2, 3$ or A_{ij}, $1 \leq i, j \leq 3$, $i < j$ is unstable. According to the Routh-Hurwitz criteria this happens if at least one of the following conditions hold:

$$\begin{aligned} -\triangle_i &< 0 \quad \text{for } i = 1, 2, 3 \\ -\triangle_i - \triangle_j &< 0 \quad \text{for } 1 \leq i, j \leq 3,\ i < j \\ \triangle_{ij} &< 0 \quad \text{for } 1 \leq i, j \leq 3,\ i < j \end{aligned}$$

Substituting the terms from the matrix A to the above formulas, we find that the only condition that holds is $\triangle_{12} = f_a\, g_b - f_b\, g_a < 0$. This is the conditions 4). Thus the conditions $1) - 4)$ ensure that the homogeneous steady state is stable without diffusion and that it is possible to find such diffusion coefficients for which the system undergoes Turing instability. To finish the proof it remains us to show that conditions 5) and 6) ensure instability of the steady state (a_s, b_s, c_s) when the diffusion is present.

Part 2. Conditions $5) - 6)$.

Now we consider the full reaction-diffusion system $(3.24) - (3.26)$ linearised about the steady state:

$$\mathbf{w}_t = A\mathbf{w} + D\Delta\mathbf{w}\,, \quad \text{in } \Omega \tag{3.32}$$

$$\mathbf{n}\cdot\nabla\mathbf{w} = 0 \quad \text{on } \partial\Omega \tag{3.33}$$

$$\mathbf{w}(\mathbf{x}, 0) = 0 \quad \mathbf{x} \in \Omega\,, \tag{3.34}$$

where D is the matrix of diffusion coefficients given by

$$D = \begin{pmatrix} D_a & 0 & 0 \\ 0 & D_b & 0 \\ 0 & 0 & D_c \end{pmatrix}.$$

As we explained in the previous section, since we assume the existence of the eigenvalue vector $\mathbf{W}(\mathbf{x})$ of the eigenvalue problem $(3.11) - (3.12)$, it is sufficient to investigate the instability of the

$$\begin{aligned} \mathbf{w}_t &= (A - Dk^2)\mathbf{w} \quad \text{in } \Omega\,, \\ \mathbf{n}\cdot\nabla\mathbf{w} &= 0 \quad \text{on } \partial\Omega\,, \\ \mathbf{w}(\mathbf{x}, 0) &= 0 \quad \mathbf{x} \in \Omega\,. \end{aligned}$$

Let us denote by λ the eigenvalues associated to the matrix $C := A - k^2 D$. Then we would like to show that $Re(\lambda(k)) > 0$ for some $k \neq 0$. The case $k = 0$ is already included in the Part 1 of this proof, because $k = 0$ removes diffusion terms from our equations, thus the system (3.32) takes the form of (3.9). From the following expression

$$\det \begin{pmatrix} D_a k^2 - f_a + \lambda & -f_b & -f_c \\ -g_a & D_b k^2 - g_b + \lambda & 0 \\ 0 & -h_b & D_c k^2 - h_c + \lambda \end{pmatrix} = 0$$

we obtain a characteristic polynomial associated to the matrix C given as:

$$P(\lambda) \;=\; \lambda^3 + c_1\lambda^2 + c_2\lambda + c_3,$$

where coefficients c_i, $i = 1, 2, 3$, are defined by (3.23), namely

$$\begin{aligned}
c_1 &= k^2(D_a + D_b + D_c) - f_a - g_b - h_c \\
c_2 &= k^4(D_aD_b + D_aD_c + D_bD_c) - k^2\left[f_a(D_c + D_b) + g_b(D_a + D_c) + h_c(D_a + D_b)\right] \\
&\quad + f_a\, h_c + g_b\, h_c + f_a\, g_b - f_b\, g_a \\
c_3 &= k^6(D_a\, D_b\, D_c) + k^4(-D_b\, D_c\, f_a - D_a\, D_c\, g_b - D_a\, D_b\, h_c) + \\
&\quad + k^2(D_c\,(f_a\, g_b - f_b\, g_a) + D_a\, g_b\, h_c + D_b\, f_a\, h_c) + f_b\, g_a\, h_c - \\
&\quad - f_a\, g_b\, h_c - f_c\, g_a\, h_b.
\end{aligned}$$

Then the Routh-Hurwitz criteria implies that matrix C is unstable if at least one of the following conditions hold:

$$c_1 < 0\,, \quad c_3 < 0 \quad \text{or} \quad c_1c_2 < c_3.$$

With the help of the conditions $1) - 3)$ and (3.30) we obtain that c_1 and c_2 are always positive, moreover they imply that $c_1c_2 > c_3$. Thus the only way as the instability can be reached is if $c_3 < 0$. In this case the Descartes sign rule implies that the polynomial $P(\lambda)$ has exactly one positive real root. Thus we need to find conditions which ensure that c_3 is negative. We rewrite c_3 as

$$c_3(k) = Ak^6 + Bk^4 + Ck^2 + D\,,$$

where coefficients A, B, C and D are defined in the conditions 6) of this theorem. Conditions $1) - 3)$ and (3.30) implies that A, B and D are positive. Since $A > 0$ then $c_3(k) \to \infty$ for $k \to \pm\infty$. In the Figure 3.1 we sketch c_3 as the function of k. Thus if c_3 is negative for some k's, there need to exists a local minimum k_{min}, such that $c_3(k_{min}) < 0$. Derivation of c_3 with respect to k^2 shows that

$$k^2_{min} = \frac{-B + \sqrt{B^2 - 3AC}}{3A}. \tag{3.35}$$

Since k is considered to be real and non-zero we obtain that $C \leq 0$. This corresponds exactly to condition 5). Since $c_3(k_{min}) < 0$ and $c_3(k) \to \infty$ for $k \to \pm\infty$, it is clear that there exit a finite range interval $[k_1, k_2]$, such that $c_3(k_1) = c_3(k_2) = 0$ and $c_3(k) < 0$ for $k \in [k_1, k_2]$. So the condition 6) is proved and so is the theorem. □

Remark. To check if the system (3.24) − (3.26) meets the condition 6) it is sufficient to verify that the minimum of $y(k)$ is negative, i.e

$$y(k_{min}) = 2B^3 - 9ABC - 2(B^2 - 3AC)^{3/2} + 27A^2D \tag{3.36}$$

where k_{min} is obtained from (3.35).

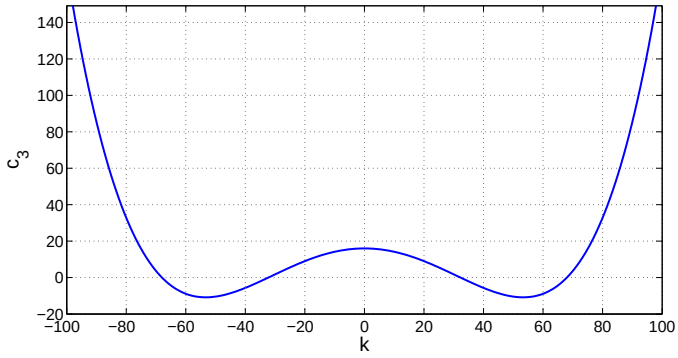

Figure 3.1: *A sketch of the coefficient c_3 as the function of k.*

Remark. Conditions 1), 2) , 3) and 5) imply that at least one of the diffusion coefficients must be different. Indeed, if $D_a = D_b = D_c$ then the condition 5) gives

$$f_a\, g_b - f_b\, g_a + g_b\, h_c + f_a\, h_c \leq 0.$$

However conditions 1), 2) and 3) imply that this expression is strictly positive. Thus one cannot have a Turing instability with identical diffusion coefficients.

Remark. It is possible to find exact formulas for eigenvalues k_1 and k_2. They can be found as roots of the polynomial $y(k)$, but they are given by a complicated expression from which little insight can be gained. To prove the Theorem 5 we do not need to know these expressions, however one will need them to determine the interval of possible wavenumbers. In such a case we recommend to use a numerical software to find roots of $y(k)$. However if someone prefers an analytical approach, we present formulas for roots of $y(k)$ in Appendix A.1.

Simulation of the illustrative model

Let us consider the illustrative model given by equations (3.24) − (3.28). We choose reaction rate constants as follows $k_1 = 1\ \mu m^3 sec^{-1}$, $k_2 = 1\ sec^{-1}$, $k_3 = 2\ \mu m^3 sec^{-1}$, $k_4 = 1\ \mu m^{-3}\, sec^{-1}$, $k_5 = 2\ sec^{-1}$ and $k_6 = 3\ \mu m^{-3} sec^{-1}$. Then the homogeneous steady state is $(a_s, b_s, c_s) = (2\,, 4\,, 0.375)\ \mu m^2 sec^{-1}$. We can immediately see that the conditions 1) − 4) hold. The condition 5) implies

$$8D_a + 48D_b - D_c < 0.$$

Thus if we fix $D_a = 0.0001\ \mu m^2 sec^{-1}$ and $D_b = 0.00001\ \mu m^2 sec^{-1}$, then we need to choose $D_c > 0.0013\ \mu m^2 sec^{-1}$. Using the condition (3.36) we obtain $D_c > 0.0128\ \mu m^2 sec^{-1}$. It means the considered systems undergoes Turing instability if $D_c > 0.0128\ \mu m^2 sec^{-1}$. We will analyse this model at first in a one dimensional domain and then in two dimensions.

One dimensional case:
Let us consider that the illustrative model (3.24) – (3.26) evolves in the interval $[0, 1]$ μm. In Figure 3.2 we plot numerically computed solution of this system for different values of the diffusion coefficient D_c. As the initial condition we choose the homogeneous steady state (a_s, b_s, c_s) with some small additive random noise. This can be implemented as follows

$$(a_0, b_0, c_0) = (a_s, b_s, c_s) + 0.01\eta,$$

where η is a random number uniformly distributed in the unit interval $(0, 1)$. The graphs of A (blue line), B (green line) and C (red line) are plotted at time $t = 1000$ sec and can be practically considered as steady states. As we expected no spatial patterns occur when $D_c < 0.0128$ $\mu m^2 sec^{-1}$. If $D_a = D_b = D_c$ then we obtain the same results as for $D_c = 0.01$ $\mu m^2 sec^{-1}$, therefore we do not plot it there.

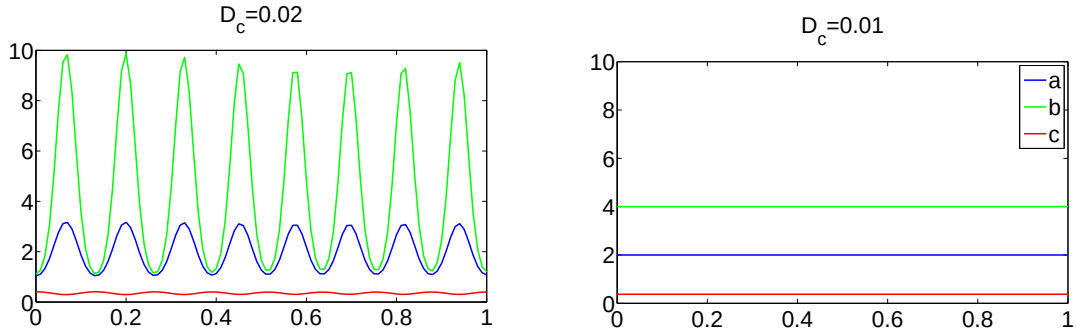

Figure 3.2: *Solution of equations* (3.24) – (3.28) *for* $D_a = 0.0001$ $\mu m^2 sec^{-1}$, $D_b = 0.00001$ $\mu m^2 sec^{-1}$ *and* $D_c = 0.02$ $\mu m^2 sec^{-1}$ *(left figure), resp.* $D_c = 0.01$ $\mu m^2 sec^{-1}$ *(right figure), at* $t = 1000$ sec *with an initial condition being the uniform steady state with small additional noise and with reaction rates specified above. We plot A (blue line), B (green line) and C (red line) in the same picture.*

If we solve equations (3.24) - (3.28) analytically in the general domain $x \in [0, L]$, $t \in [0, \infty)$ we find that the separable solution is of the form

$$\mathbf{w}(x, t) = \sum_k c_k \exp(\lambda t) \cos(kx),$$

where the sum is over the allowed values of k i.e.

$$k = \frac{n\pi}{L}, \quad n \in \{1, 2, ...\}, \tag{3.37}$$

and c_k is k-dependent in general but independent of t and x.

Influence of the domain size

The equation (3.37) may bring us to an idea that the Turing instability is also influenced by the size of the domain. More specifically, if the smallest allowed value of $k = \pi/L$ is such that

$$k = \frac{\pi}{L} > k_2$$

then we cannot have the Turing instability. Thus for such small domains that $L < L_{ctit} = \pi/k_2$, there is no pattern formation via the Turing mechanism. For instance the illustrative model, with $D_c = 0.02\ \mu m^2\,\mathrm{sec}^1$ and other parameters defined above, undergoes the Turing instability for

$$k \in [k_1,\, k_2] = [32.2794\,,\, 67.9955]$$

and the critical domain size is $L_{crit} = 0.04620\ \mu m$.

Number of Patterns

In the previous section, we mentioned that $\omega = 2\pi/k$ is a wavelength. It means that for the given size of the domain we can find the corresponding number of patterns. If we consider one dimensional domain of length L, then the number of patterns, i.e peaks, is

$$n = \frac{L}{\omega} = \frac{Lk}{2\pi}\,, \quad \text{for } k \in [k_1,\, k_2]. \tag{3.38}$$

Choosing $k = k_1$ and $k = k_2$ we obtain that possible number of patterns for the system is given as $n \in [\frac{k_1 L}{2\pi}\,,\, \frac{k_2 L}{2\pi}]$. Since n is considered as a number of patterns it seems reasonable to assume it as a positive integer. However as we can see on the Figure 3.3 the system may produce just a part of a peak. If we, for instance, define $n = 0.5 \times l$, where l is positive integer, then we find that the possible number of peaks for the illustrative model in the domain of length 1 μm is within the interval $n \in [5\,, 10.5]$.

Robustness

Let us note that the systems with Turing instability are not robust enough. It means that even a small change in the initial conditions may lead to qualitatively different solutions. For instance, on Figure 3.3 we plot the one dimensional solution of the system (3.24) − (3.28) for the same values of reaction rates and diffusion coefficients. We simply change the generator of random numbers, it means we slightly change the initial conditions. In the deterministic models, it means models described by concentration, once the system reaches the state with

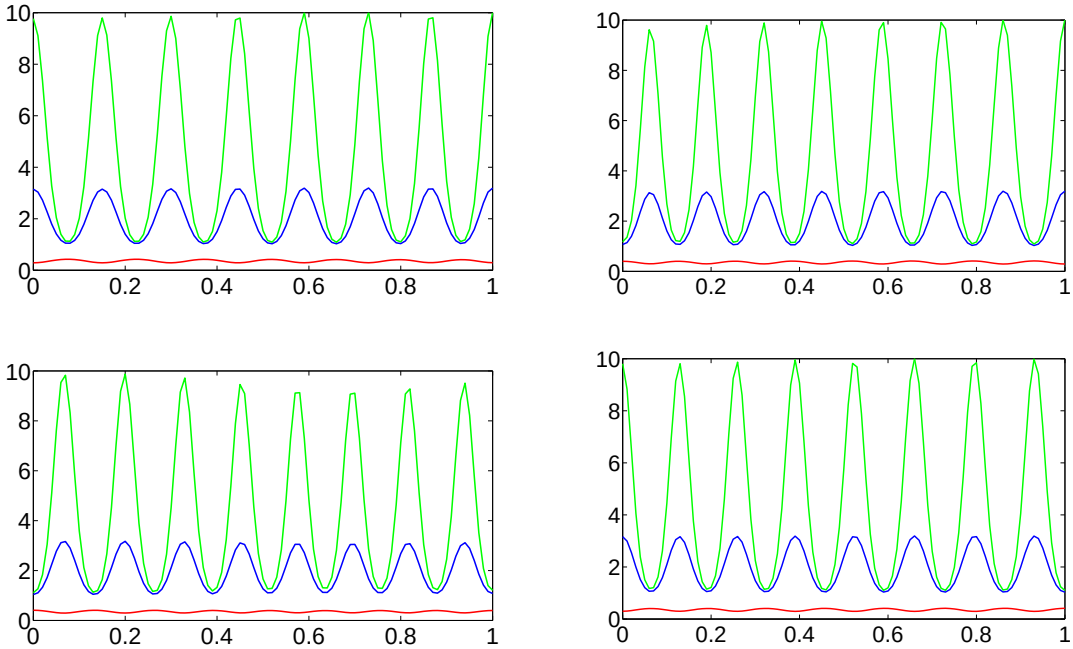

Figure 3.3: *Solution of Eqs.* (3.24) - (3.28) *with the initial condition being the perturbed uniform steady state. In all three cases we use the same values for diffusion coefficients and reaction rates. Different results are caused by the change of the generator of random numbers, which corresponds to a small change in the initial conditions. We plot A (blue line), B (green line) and C (red line) in the same picture.*

given number of patterns, it will stay there. As we will see in the following chapters, the systems with small number of molecules may switch between states with different numbers of peaks.

This model sensitivity to small perturbation might create the impression that the Turing model is inappropriate when applied to robust pattern formation in developmental biology. However the main characteristic of the development is the growth. Crampin at al. [32] showed that the domain growth could be used to select robustly certain types of patterns. Kondo and Asai [17] showed that Turing mechanisms can correctly predict future patterns on the marine angelfish skin. This pattern formation is different as then the one on the mammalian coat, which enlarge proportionally during the body growth. This is contrary to the patterns on the marine fish which maintain the space between the stripes by the continuous rearrangement of the patterns.

Two Dimensional Case:

Let us assume that the system evolves in the two-dimensional domain $[0, 0.5]\ \mu m \times [0, 0.5]\ \mu m$ with the following diffusion coefficients $D_a = 0.0001\ \mu m^2 sec^{-1}$, $D_b = 0.00001\ \mu m^2 sec^{-1}$ and $D_c = 0.02\ \mu m^2 sec^{-1}$. In Figure 3.4 we plot numerically computed solution of this system with the initial condition being the perturbed

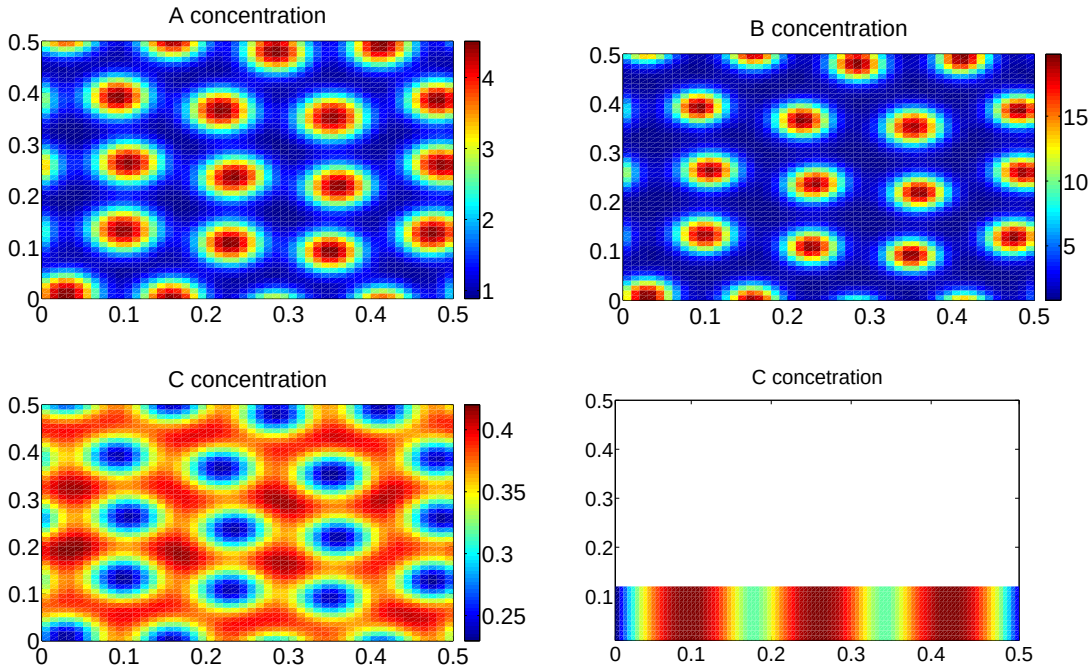

Figure 3.4: *Solution of Eqs.* (3.24) - (3.28) *in two dimensional domain with the initial condition being the perturbed uniform steady state. In first three figure is concentration of A, B and C, respectively, in a square domain* $[0\,, 0.5]\ \mu m \times [0,\ 0.5]\ \mu m$. *In last figure is concentration of C molecules in a narrow domain* $[0\,, 0.5]\ \mu m \times [0,\ 0.1]\ \mu m$.

uniform steady state. Concentrations are plotted at time $t = 1500\,\text{sec}$ and can be practically considered as steady states. The system starts to evolve from the state close to the homogeneous steady state and evolves till it reaches stable patterns. On Figure 3.5 we present the evolution of concentration of A molecules. For better illustration, please see attached movie called Turing.avi or download it from *http://tdo.sk/∼jana/Turing.avi*.

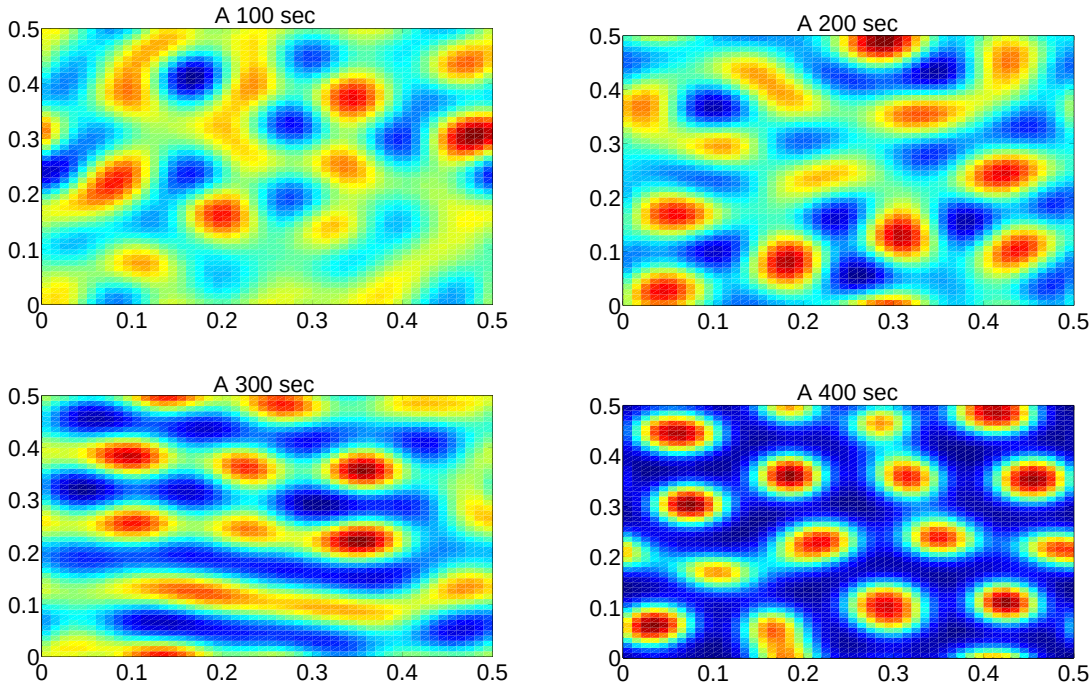

Figure 3.5: *Evolution of the concentration of molecules of A. We solve equations* (3.24) – (3.28) *with the initial condition being the perturbed uniform steady state and plot the concentration of molecules of A at different times.*

If we search for an analytical solution in the general domain $[0, a] \times [0, b]$ we find that the allowed values of k^2 are

$$k^2_{m,n} = \left[\frac{m^2\pi^2}{a^2} + \frac{n^2\pi^2}{b^2}\right]$$

and separable solution is

$$\mathbf{w}(\mathbf{x}, t) = \sum_{m=0}^{\infty}\sum_{n=0}^{\infty} c_{l,m} \exp(\lambda t) \cos\left(\frac{m\pi x}{a}\right) \cos\left(\frac{n\pi y}{b}\right),$$

where $c_{l,m}$ is independent of t and $\mathbf{x}$.

Influence of the domain size

Now we look how the size of domain influence on the formation of patterns in the two-dimensional case. If the domain is long and thin, $b \ll a$, we may have a Turing instability if

$$k^2_{m,n} = \left[\frac{m^2\pi^2}{a^2} + \frac{n^2\pi^2}{b^2}\right] \in \left[k_1^2, k_2^2\right].$$

Thus for b sufficiently small, this requires $n = 0$ and therefore no spatial variation would develop in the y direction. This typically invokes striped patterns. In Figure 3.4 in the right bottom we plot concentration of C molecules in narrow

domain $[0\,,\ 0.5]\ \mu m \times [0\,,\ 0.1]\ \mu m$.
For a large rectangular domain, $b \sim a$ sufficiently large, it is clear that the Turing instability can be initiated with $n, m > 0$. It means spatial variation would develop in both directions x and y. This typically invokes a spotted patterns, which are plotted in Figure. (3.4).

Remark. (Numerical Method)
To solve the system of partial differential equations $(3.24)-(3.28)$ we use the spectral method, which is built on the same idea as the finite element method. The main difference is that the spectral method approximates the solution as a linear combination of continuous functions that are generally nonzero over the domain of the solution (usually sinusoids or Chebyshev polynomials), while the finite element method approximates the solution as a linear combination of piecewise functions that are nonzero on small subdomains. Because of this, the spectral method takes on a global approach while the finite element method is a local approach. This is part of why the spectral method works best when the solution is smooth [41].

3.4.1 Mammalian Coat Patterns

In this part we will study perhaps the most spectacular example of the pattern formation, mammalian coat pattering. This pattern formation is described as a reaction-diffusion system, where some chemical species stimulates production of melanin[2] and some inhibits its production. We will model mammalian body as a domain which changes its aspect ratio from rectangular to long and thin. If we assume that patterns on mammals are driven by Turing instabilities then we have following possibilities[3]:

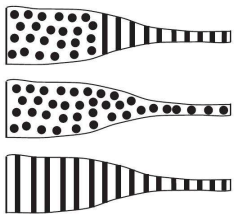

Figure 3.6: *Possibilities of mammals coat pattering by the Turing instability.*

Common observation is consistent with our assumption (see Figure 3.7) but one should not expect universal laws in the realms of biology as one does in physics [11] (see Figure 3.8). More generally this analysis has applications in modelling numerous chemical and biochemical reactions, in vibrating plate theory, and studies of patchiness in ecology and modelling gene interactions.

[2]Melanin is a substance that gives the skin and hair its natural color.
[3]Figure reproduced with permission from [11]

Figure 3.7: *Animal coat markings which are consistent with the prediction of pattern formation by the Turing instability.*

Figure 3.8: *Animal coat markings which are inconsistent with the prediction of pattern formation by the Turing instability.*

3.4.2 Schnakenberg system

Let us note that under certain conditions, the illustrative model, defined in the first chapter, provides a good approximation of system studied by Schnakeberg [61]. This is a reaction-diffusion system of two chemical species, let's say A and C, which diffuse with diffusion coefficients $\tilde{D}_a$ and $\tilde{D}_c$ and react according to

$$2A + C \overset{m_1}{\to} 3A \tag{3.39}$$

$$\emptyset \overset{m_2}{\to} A \tag{3.40}$$

$$A \overset{m_3}{\to} \emptyset \tag{3.41}$$

$$\emptyset \overset{m_4}{\to} C, \tag{3.42}$$

where the m_1, m_2, m_3 denotes reaction rates. The Schnakenberg system was used in the model of the follicule spacing on the skin of mice, presented by Sick et al [12]. It is also used in the simulation of mammalian coat pattering studied in [1]. Now let us explain how the two-component Schnakenberg system can be approximated by the three component illustrative model defined in the first chapter. If $m_2 = k_4$, $m_3 = k_5$, $m_4 = k_6$, $\tilde{D}_a = D_a$ and $\tilde{D}_c = D_c$, then chemical reactions $(3.40) - (3.42)$ are exactly the same reactions as $(2.3) - (2.5)$. The reaction (3.39) can be approximated by $(2.1) - (2.2)$ if we assume that the B molecules exist in the system only for a short amount of time. Furthermore, this assumption implies that the concentration for B is never large, it means that the bulk of the mass is shared between species A and C which is to be expected for the two component Schnakenberg system. The assumption on the short life time of B molecules holds if k_2 and k_3 are large. Thus we introduce a small parameter

$\varepsilon > 0$ such that $1/\varepsilon = k_2$. Then the comparison of the total mass of both models implies, that these two models are equivalent if

$$k_1 = \rho m_1,$$

where $\rho = k_3/k_2$, such that $\rho << 1/\varepsilon$ and if $D_b = 0$. The assumption on the diffusion constant D_b matters because the concentration of B is small everywhere. It means that the b is small and so is the diffusion term.

The reaction-diffusion mechanism of the Schnakenberg model is governed by the following equations

$$\frac{\partial a}{\partial t} = \tilde{D}_a \Delta a + f(a, c) \tag{3.43}$$

$$\frac{\partial c}{\partial t} = \tilde{D}_c \Delta c + g(a, c), \tag{3.44}$$

where f and g stands for the corresponding reaction terms. The conditions under which this system undergoes Turing instability are presented in the following theorem.

Theorem 6. *(Conditions for Turing Instability of the Schnakenberg system) The diffusion-driven instability of the system* (3.39)-(3.42) *occurs if the following inequalities hold:*

$$f_a + g_c < 0\,, \tag{3.45}$$
$$f_a g_c - f_c g_a > 0\,, \tag{3.46}$$
$$\tilde{D}_c f_a + \tilde{D}_a g_c > 0\,, \tag{3.47}$$
$$\left(\tilde{D}_c f_a + \tilde{D}_a g_c\right) > 2\sqrt{\tilde{D}_a \tilde{D}_c \left(f_a g_c - f_c g_a\right)}\,. \tag{3.48}$$

And if there exists a time-independent solution $\boldsymbol{W}(\boldsymbol{x})$*, of spatial eigenvalue problem* (3.11) − (3.12) *with eigenvalue* k^2*,* $(k \in \mathbb{R})$ *within the following range*

$$k^2 \in \left[\frac{A - \sqrt{A^2 - B}}{2\tilde{D}_a \tilde{D}_c}, \frac{A + \sqrt{A^2 - B}}{2\tilde{D}_a \tilde{D}_c}\right],$$

where

$$A = \tilde{D}_c f_a + \tilde{D}_a g_c,$$
$$B = 4\tilde{D}_a \tilde{D}_c (f_a g_c - f_a g_c).$$

The idea of the proof is the same as in the proof of Theorem 5, but it is easier since the Schnakenebrg system deals only with two chemical species. The proof can be found in [1] or [11].

Model specification

In all simulations of the illustrative model we will use following diffusion coefficients and the following reaction rates

$$D_a = 1 \times 10^{-4}\ \mu m^2 sec^{-1}, \quad D_b = 1 \times 10^{-5}\ \mu m^2 sec^{-1}, \tag{3.49}$$
$$D_c = 0.02\ \mu m^2 sec^{-1}, \quad k_1 = 1\ \mu m^3 sec^{-1}, \tag{3.50}$$
$$k_2 = 1\ sec^{-1}, \quad k_3 = 2\ \mu m^3 sec^{-1}, \tag{3.51}$$
$$k_4 = 1\ \mu m^{-3} sec^{-1}, \quad k_5 = 2\ sec^{-1} \tag{3.52}$$
$$k_6 = 3\ \mu m^{-3} sec^{-1}. \tag{3.53}$$

Similar, we specify the model parameters for the *Schnakenberg model*

$$\tilde{D}_a = 5 \times 10^{-4}\ \mu m^2 sec^{-1}, \quad \tilde{D}_c = 0.06\ \mu m^2 sec^{-1} \tag{3.54}$$
$$m_1 = 1\ \mu m^4 sec^{-1}, \quad m_2 = 1\ \mu m^{-2} sec^{-1}, \tag{3.55}$$
$$m_3 = 2\ sec^{-1}, \quad m_4 = 3\ \mu m^{-2} sec^{-1} \tag{3.56}$$

One can easily check that this model fulfils conditions from Theorem 6.

4. Compartment-based Stochastic Reaction-Diffusion Algorithm

In the previous chapter we studied pattern formation in the systems characterised by concentration and described by the partial differential equations. If we want to explore this process at the molecular level, we need to describe the system by number of molecules rather then by concentrations and use the stochastic approach instead of the deterministic one.

In this chapter we study one of the compartment based stochastic simulation algorithms. The idea of this algorithm is to divide the domain into small compartments, such that molecules within each compartment are well mixed. It is not necessary for molecules to be well-mixed between the compartments. Furthermore we will assume that only molecules in the same compartment may react. Since molecules are well-mixed we can use the Gillespie algorithm to simulate chemical reaction within each compartment. Moreover, thanks to the division of the domain, we can incorporate the diffusion to the system as follows.

For simplicity let us at first consider a one dimensional domain of the length L divided into K compartments of the length $h = L/K$ (see Figure 4.1a). To describe the diffusion of molecules of chemical species A within this domain, we denote the number of A molecules in the i-th compartment $[(i-1)h\,,\, ih)$ by A_i, $i = 1, \ldots, K$. As a result of the Brownian motion particles naturally cross from one imaginary compartment to another (see Figure 4.2). These jumps between neighbouring compartments can be simulated as a chain of chemical reactions [23, 7, 54] :

$$A_1 \underset{d}{\overset{d}{\rightleftarrows}} A_2 \underset{d}{\overset{d}{\rightleftarrows}} A_3 \underset{d}{\overset{d}{\rightleftarrows}} \ \ldots \ \underset{d}{\overset{d}{\rightleftarrows}} A_K. \tag{4.1}$$

Since all molecules can diffuse to the right with the same probability as to the left, all above chemical reactions occur with the same reaction rate d. We

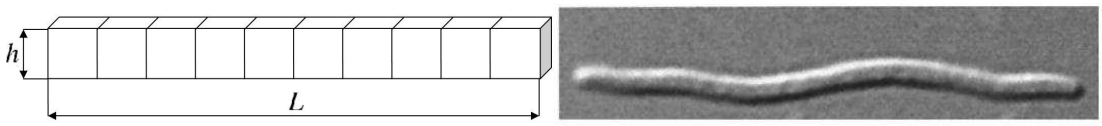

(a) (b)

Figure 4.1: *(a) Domain* $[0, L]$ *divided into* K *compartments. Diffusion is considered only from left to the right and vice versa. (b) A snapshot of E. coli, presented in [16].*

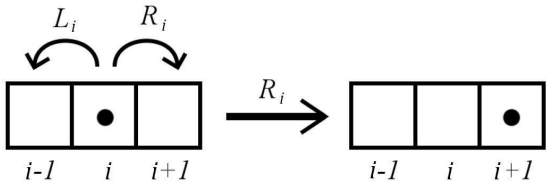

Figure 4.2: *Diagram illustrating the stochastic description of diffusion. Each particle has equal probability of moving left as moving right. If for example, the right diffusion reaction, R_i, occurs one molecule from box i moves to box $i+1$. Reproduced from [44]*

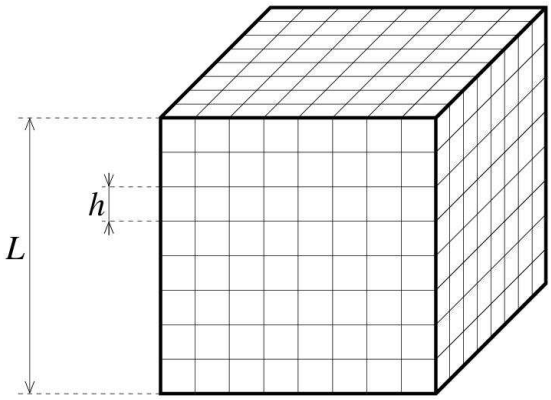

Figure 4.3: *Domain $[0, L]^3$ is divided into K^3 compartments. Reproduced from [6]*

can use the Gillespie algorithm to simulate chemical reactions in (4.1). The only parameter that needs to be determined is the rate constant d. It can be shown, ([7], Chapter 5.), that the Gillespie algorithm is the correct model of diffusion provided that the rate constant d in (4.1) is chosen as

$$d = \frac{D}{h^2}, \tag{4.2}$$

where D is the diffusion constant. It is easy to extend this model of diffusion for two or three dimensions by dividing the corresponding domain in compartments (see Figure 4.3) and allow the molecules to jump in any of the adjacent four, respectively six, compartments.

The compartment based models were recently implemented to the MesoRD [23] and to the SmartCell [40] simulators. For instance the reaction-diffusion processes needed for the division of *E. coli* [16] was modelled using the MesoRD simulator.

Now let us properly explain the compartment based model on the three component illustrative model in general three dimensional domain. To do this we inherit the notation presented in [6].

4.1 Compartment-Based Simulation of the Illustrative Model

Let us assume that the chemical species A, B and C, from the illustrative model, diffuse with diffusion coefficients D_a, D_b and D_c, respectively, in the cubic container $[0, L]^3$. We incorporate this domain with zero flux (reflective) boundary conditions, i.e. whenever a molecule hit the boundary, it is reflected back. For implementation of more specific boundary conditions see Erban and Chapman paper [5]. We divide the domain $[0, L]^3$ into K^3 cubic compartments of volume h^3, where $h = L/K$ and $K \geq 1$ (see Figure 4.3). We will denote the compartments by indices from a set [6]

$$I_{all} \;=\; \{(i,j,k)|\; i,\, j,\, k \text{ are positive integers such that } 1 \leq i,j,k \leq K\}\,.$$

The number of molecules A, B, resp. C in the (i, j, k)-th compartment at time t is denoted as $A_{ijk}(t)$, $B_{ijk}(t)$, resp. $C_{ijk}(t)$, where $(i, j, k) \in I_{all}$. Diffusion of these molecules is modelled as a jump process between neighbouring compartments. Therefore we define the set of all possible directions of the diffusion jumps as follows [6]:

$$E \;=\; \{[1,\,0,\,0],\; [-1,\,0,\,0]\,, [0,\,1,\,0]\,, [0,\,-1,\,,0]\,, [0,\,0,\,1]\,, [0,\,,0\,,-1]\}\,.$$

For each compartment $(i\,, j\,, k) \in I_{all}$ we define the set of all possible directions of jumps from this compartment [6]:

$$E_{ijk} \;=\; \{\mathbf{e} \in E|\,(\,(i,\,j,\,k) + \mathbf{e}) \in I_{all}\}.$$

Then the illustrative model can be rewritten as a system of $3K^3$ "chemical species" A_{ijk}, B_{ijk} and C_{ijk}, where $(i,\, j,\, k) \in I_{all}$ which are subject to the following chemical reactions:

$$A_{ijk} + A_{ijk} \;\overset{k_1}{\rightarrow}\; B_{ijk} \tag{4.3}$$

$$B_{ijk} \;\overset{k_2}{\rightarrow}\; A_{ijk} + A_{ijk} \tag{4.4}$$

$$B_{ijk} + C_{ijk} \;\overset{k_3}{\rightarrow}\; B_{ijk} + A_{ijk} \tag{4.5}$$

$$\emptyset \;\overset{k_4}{\rightarrow}\; A_{ijk}\,, \quad A_{ijk} \;\overset{k_5}{\rightarrow}\; \emptyset\,, \quad \emptyset \;\overset{k_6}{\rightarrow}\; C_{ijk} \tag{4.6}$$

$$A_{ijk} \;\overset{D_a/h^2}{\rightarrow}\; A_{ijk+\mathbf{e}} \tag{4.7}$$

$$B_{ijk} \;\overset{D_b/h^2}{\rightarrow}\; B_{ijk+\mathbf{e}} \tag{4.8}$$

$$C_{ijk} \;\overset{D_c/h^2}{\rightarrow}\; C_{ijk+\mathbf{e}}, \tag{4.9}$$

where $(i,\, j,\, k) \in I_{all}$ and $\mathbf{e} \in E_{ijk}$. The reactions $(4.3) - (4.6)$ represent chemical reactions $(2.1) - (2.5)$ considered in each compartment. The propensity functions of these chemical reactions are the same as presented in table 2.1, but instead of

the volume of the whole domain we consider just the volume of the compartment. For instance the propensity function of (4.5) is

$$\alpha_{ijk,3} = B_{ijk}C_{ijk}k_3/h^3$$

where h^3 is the volume of the compartment. The reactions (4.7) – (4.9) represent diffusive jumps between the neighbouring compartments. Their propensity functions are given as

$$\alpha_{ijk,D_a} = A_{ijk}D_a/h^2, \quad \alpha_{ijk,D_b} = B_{ijk}D_b/h^2, \quad \alpha_{ijk,D_c} = C_{ijk}D_c/h^2.$$

Each of reactions in (4.7)−(4.9) effectively describes $6K^3-6K^2$ reactions, because each diffusing molecule has 6 possible directions to jump from each inner compartment and some directions are missing for boundary compartments [6, 7]. Thus the compartment-based model of the illustrative system is a set of $3K^3$ "chemical species" which are subject to $27K^3 - 18K^2$ reactions presented in (4.3) – (4.9). The time evolution of this system can be simulated by the Gillespie algorithm.

Remark. In a general compartment-based model it is possible to divide the domain in compartments which are not cubic and which are not of the same size [42, 43]. However in such case it may be difficult to distinguish which phenomena are genuine property of the system and which are only the consequence of the non-uniform mesh. In this thesis we use only the uniform cubic compartments, because they are the most natural choice and it is easy to implement them computationally. However it needs to be noted that the uniform cubic mesh brings an artificial anisotropy to the system, because the compartments have different length along the side and along the diagonal [6]. The potential consequences of this fact are not investigated here.

In the following sections we apply the presented compartment based model to the illustrative system. We will study two different cases. At first, we show that under certain conditions the compartment based SSA provides the same results as the deterministic model. In the second case we will investigate the stochastic behaviour in the system.

4.2 Compartment-Based Model in the "Deterministic Limit"

It can be shown [53], if the number of molecules in the system tends to infinity and if the size of the compartment $h \to 0_+$ then the system of equations (4.3) – (4.9) is well approximated by the system of PDEs (3.24) – (3.26). We verify this by numerical simulations. To do this we will consider the illustrative

system with large number of molecules in the domain divided into large number of compartments. The term "large number" is related to the size of the domain. At first let us consider the illustrative model within a "one dimensiona" domain of the length $L = 1\ \mu m$ divided into $K = 100$ compartments of the size $h = L/K$ (see Figure 4.1a). Although it may seems useless to study behaviour of such domain the opposite is true. Firstly this domain is actually three dimensional domain $[0, L] \times [0, h] \times [0, h]$. The name "one dimensional" refers to the fact that the diffusion is considered only from right to left and vice versa. To remove the feeling this is an artificial concept, let us note that a similar type of domain was used to simulate the division of *E. coli* [16]. This dividing process is governed by so called Min proteins which diffuse between poles of a bacteria and which role is to specify the middle point of the bacteria to ensure a symmetrical division. In this situation it is appropriate to consider an elongate domain with one dimensional diffusion. In the Figure 4.1 we present a snapshot of *E. coli* in a comparison with the "one-dimensional" domain.
Furthermore we need to considered a large number of molecules in the system. To do this we will assume that the number of molecules per compartment is of the order 1000. This can be achieved by appropriate rescaling of the reaction rate constants (see Section 2.2). Since the volume of a single compartment is $\nu := h^3 = 10^{-6}\mu m^3$ and we want to have 1000 molecules per compartment, following rescaling of reaction rates is needed:

$$\begin{aligned} k_1 = 1/1000, \quad k_2 = 1, \quad k_3 = 2/1000 \\ k_4 = 1000, \quad k_5 = 2, \quad k_6 = 3000. \end{aligned} \tag{4.10}$$

In the Figure 4.4 we present results of compartment-based simulation in the "one dimensional domain" $[0, 1]\ \mu m \times [0, 0.01]\ \mu m \times [0, 0.01]\ \mu m$. We initially consider 2000 molecules of A, 4000 molecules of B and 370 molecules of C in each compartment, i.e. at the beginning of simulation we set $A_i(0) = 2000$, $B_i(0) = 4000$ and $C_i(0) = 370$, for $i = 1, \ldots, K$. We let the system evolve for 10000 *sec.* Presented results correspond to the one dimensional deterministic solutions presented in Chapter 3. The system starts to evolve from the homogeneous state and similarly as in the deterministic case once the state with a specific number of patterns (peaks) is reached, the system stays there. In Figure 4.4d we plot the number of peaks of A molecules as a function of time. As we can see no switching between states with different number of peaks is observed.

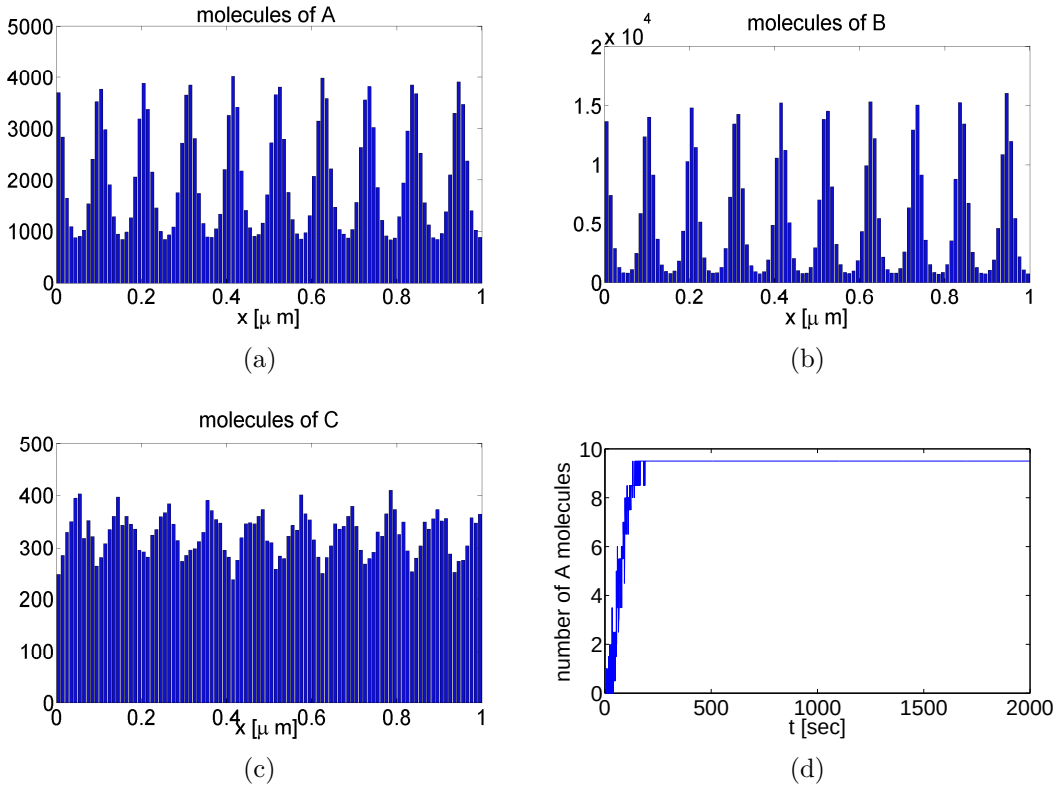

Figure 4.4: *(a)-(c) Stochastic simulation of the illustrative model in* $[0, 1]$ μm *domain divided into* $K = 100$ *compartments. The diffusion coefficient and reaction rates given by* $(3.49) - (3.53)$*. We initially place* 2000 *molecules of* A*,* 4000 *molecules of* B *and* 370 *molecules of* C *in each compartment and let the system evolve for* 10000 *sec. (d)The time evolution of the number of patterns (peaks) of* A *molecules.*

Now we will consider the illustrative model in the "two-dimensional" domain $[0, L] \times [0, L] \times [0, h]$, where $L = 0.2\ \mu m$ and $h = 0.01 \mu m$. More precisely, it is three dimensional domain in which particles diffuse along two coordinates. We use the same reaction rates as in the "one-dimensional" case. The initial conditions are choose as follows i.e. $A_{i,j}(0) = 2000$, $B_{i,j}(0) = 4000$ and $C_{i,j}(0) = 370$, for $i, j = 1, \ldots, K$ In figure 4.5 we present a result of the compartment-based simulation in the comparison with the deterministic solution.

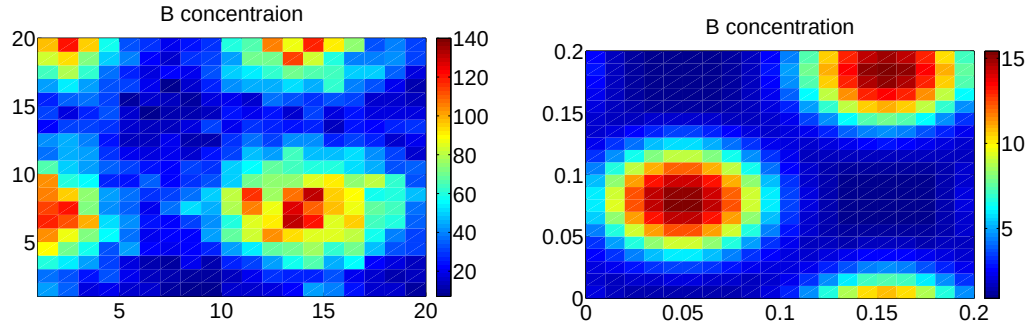

(a) (b)

Figure 4.5: *(a) Stochastic simulation of the illustrative model in the domain* $[0, 2]\ \mu m \times [0, 2]\ \mu m \times [0, 0.01]\ \mu m$ *divided into* 20×20 *compartments. (b) Deterministic solution of the equations* (2.16) – (3.26) *in the domain* $[0, 0.2]\ \mu m \times [0, 0.2]\ \mu m$.

To obtain a better resolution for the compartment-based model we need to increase the number of compartments, but it implies an increase in the number of "chemical species". Since the compartment based model is based on the Gillespie algorithm this would also increase the computational time. An improvement can be achieved if the Gillespie algorithm is replaced by the next subvolume method or the next reaction method. These methods scales logarithmically with the number of compartments, whereas the Gillespie algorithm scales linearly. Although we do not use these methods in this thesis, we briefly explain them, to provide some guidance for increasing the efficiency of the compartment based model.

The *next reaction method*, is the method implemented in the SmartCell simulator. It works similarly as the presented compartment based algorithm, but instead of the Gillespie algorithm it uses a Gibson-Bruck algorithm [45]. This algorithm can be explained as follows. After the initialisation of molecules, we compute the propensity function for each event i.e. for each possible reaction and diffusion. Moreover, for each of them we compute and store the time when the next event occurs. Then the event with the smallest next occurrence time is chosen and evaluated. After this we recompute the propensity functions and the next event time only for those events which were changed in the previous step. Then the process is repeated. One advantage of this concept is that we do not

need to compute all propensity functions in each time step as it is in the Gillespie algorithm. Moreover, we do not need to generate so many random numbers.
The next subvolume method, implemented in the MesoRD simulator, can be described as follows. At the beginning we define a domain, divide it into compartments and distribute the initial numbers of molecules into the compartments. Then we compute the propensity function for each compartment as the sum of the propensity functions of all possible events within the compartment. Moreover, for each compartment we compute the next event time. Then we order the compartments according to their next event times, such that the compartment with the lowest next event time is on the top of the queue. Inside of the compartment, which is at the top of the queue, we find the event which will occur in the next time step and update the state of the system according to this. For compartments, whose state is changed by this event, we recompute the propensity function and the next event time. Then we insert them into the queue, order the queue and repeat the processes above. The advantage of this method is that we can quickly find the compartment within the next event occurs. Similar to the next reaction method we recompute only those propensity functions and those next event times which were changed in the previous step. This saves time and random numbers.

4.3 Stochastic Behaviour

In this section we will study the behaviour of the system out of the deterministic limit, i.e. we will consider the system with a small number of compartments and molecules. At this moment a question arise what the term "small number" means. Since the number of molecules is usually determined by the reality and thus it is not in hands of modellers, we would not focus so much on it. Our attention is focused on the only model parameter, i.e. the number of compartments K. To answer the question what should be considered as a small number of compartments, we will search for the minimal number of compartments within which the Turing instability can arise. We already know that no Turing patterns are produced in the domain composed from a single compartment. It is because the compartment-based model in one compartment is equivalent to the Gillespie algorithm. As we saw in Chapter 2 no Turing patterns are produced there, because the diffusion is not considered.
In the Subsection 4.3.1 we derive the minimal number of compartments needed for Turing instability. As soon as we will know this minimal number, we start to investigate the role of the noise in the system. This is the aim of Subsection 4.3.2. Due to a simpler investigation we perform all following analysis in "one dimensional" domain.

4.3.1 Minimal Number Of Compartments

Let us consider the illustrative model in the "one-dimensional" domain. Since the number of compartments depends on the domain size we fix it at first. For simplicity we fix $L = 1\ \mu m$, i.e. the number of compartments is given as $K = 1/h$. Then the idea how the minimal number of compartments can be found is following. We can compute the homogeneous steady state for the illustrative model within one-dimensional domain divided into arbitrary number of compartments. Moreover, we know that this state is stable without diffusion. To find the minimal number of compartments in which Turing instability can arise, we search for such number of compartments K, that this steady state becomes unstable when the diffusion is presented. To decide weather the system posses an unstable steady state or not, we will investigate the eigenvalues of the corresponding Jacobian matrix.

To implement presented idea, we at first derive the form of the Jacobian matrix. For simplification, we will firstly consider the illustrative model within the domain divided into three compartments. In this case the reaction diffusion mechanism is govern by following nine equations:

$$\begin{aligned}
\frac{dA_1}{dt} &= \frac{-k_1}{h^3}A_1^2 + k_2B_1 + \frac{k_3}{h^3}B_1C_1 + k_4h^3 - k_5A_1 + \frac{D_a}{h^2}A_2 - \frac{D_a}{h^2}A_1\,,\\
\frac{dA_2}{dt} &= \frac{-k_1}{h^3}A_2^2 + k_2B_2 + \frac{k_3}{h^3}B_2C_2 + k_4h^3 - k_5A_2 + \frac{D_a}{h^2}A_1 - \frac{2D_a}{h^2}A_2 + \frac{D_a}{h^2}A_3\,,\\
\frac{dA_3}{dt} &= \frac{-k_1}{h^3}A_3^2 + k_2B_3 + \frac{k_3}{h^3}B_3C_3 + k_4h^3 - k_5A_3 + \frac{D_a}{h^2}A_2 - \frac{D_a}{h^2}A_3\,,\\
\frac{dB_1}{dt} &= \frac{k_1}{h^3}A_1^2 - k_2B_1 + \frac{D_b}{h^2}B_2 - \frac{D_b}{h^2}B_1\,,\\
\frac{dB_2}{dt} &= \frac{k_1}{h^3}A_2^2 - k_2B_2 + \frac{D_b}{h^2}B_1 - \frac{2D_b}{h^2}B_2 + \frac{D_b}{h^2}B_3\,,\\
\frac{dB_3}{dt} &= \frac{k_1}{h^3}A_3^2 - k_2B_3 + \frac{D_b}{h^2}B_2 - \frac{D_b}{h^2}B_3\,,\\
\frac{dC_1}{dt} &= -\frac{k_3}{h^3}B_1C_1 + k_6h^3 + \frac{D_c}{h^2}C_2 - \frac{D_c}{h^2}C_1\,,\\
\frac{dC_2}{dt} &= -\frac{k_3}{h^3}B_2C_2 + k_6h^3 + \frac{D_c}{h^2}C_1 - \frac{2D_c}{h^2}C_2 + \frac{D_c}{h^2}C_3\,,\\
\frac{dC_3}{dt} &= -\frac{k_3}{h^3}B_3C_3 + k_6h^3 + \frac{D_c}{h^2}C_2 - \frac{D_c}{h^2}C_3\,.
\end{aligned}$$

There the letters A_i, B_i and C_i denote the number of molecules of A, B and C in the i-th compartment, $i = 1, 2, 3$. The homogeneous steady state (A_0, B_0, C_0) of the above system is given as

$$A_0 = \frac{k_6h^3 + k_4h^3}{k_5}, \quad B_0 = \frac{k_1}{k_2h^3}A_0^2, \quad \text{and} \quad C_0 = \frac{k_6h^6}{k_3B_0}. \tag{4.11}$$

The steady state for the illustrative model within arbitrary number of compartments is also given by equations (4.11). For easier handling we express the above

nine equations governing the reaction-diffusion mechanism as follows:

$$\begin{aligned}
\frac{dA_1}{dt} &= f_1(A_1, A_2, B_1, C_1) + \frac{D_a}{h^2}A_2 - \frac{D_a}{h^2}A_1\,,\\
\frac{dA_2}{dt} &= f_2(A_1, A_2, A_3, B_2, C_2) + \frac{D_a}{h^2}A_1 - \frac{2D_a}{h^2}A_2 + \frac{D_a}{h^2}A_3\,,\\
\frac{dA_3}{dt} &= f_3(A_2, A_3, B_3, C_3) + \frac{D_a}{h^2}A_2 - \frac{D_a}{h^2}A_3\,,\\
\frac{dB_1}{dt} &= g_1(A_1, B_1, B_2) + \frac{D_b}{h^2}B_2 - \frac{D_b}{h^2}B_1\,,\\
\frac{dB_2}{dt} &= g_2(A_2, B_1, B_2, B_3) + \frac{D_b}{h^2}B_1 - \frac{2D_b}{h^2}B_2 + \frac{D_b}{h^2}B_3\,,\\
\frac{dB_3}{dt} &= g_3(A_3, B_2, B_3) + \frac{D_b}{h^2}B_2 - \frac{D_b}{h^2}B_3\,,\\
\frac{dC_1}{dt} &= h_1(B_1, C_1, C_2) + \frac{D_c}{h^2}C_2 - \frac{D_c}{h^2}C_1\,,\\
\frac{dC_2}{dt} &= h_2(B_2, C_1, C_2, C_3) + \frac{D_c}{h^2}C_1 - \frac{2D_c}{h^2}C_2 + \frac{D_c}{h^2}C_3\,,\\
\frac{dC_3}{dt} &= h_3(B_3, C_2, C_3) + \frac{D_c}{h^2}C_2 - \frac{D_c}{h^2}C_3\,.
\end{aligned}$$

Thus the reaction terms of chemical species A_i, B_i and C_i are substituted by functions f_i, g_i and h_i, respectively, where $i = 1, 2, 3$. Then the Jacobian matrix related to the three compartment system can be obtain by corresponding derivations of the above equations. Using the symmetry of these equation, we can derive the general form of the Jacobian matrix, denoted as $\mathcal{J}$. Since the illustrative model consists of three chemical species, $\mathcal{J}$ is $3K \times 3K$ matrix, where K denotes the number of compartments. Then $\mathcal{J}$ can be built from nine blocks:

$$\mathcal{J} = \begin{pmatrix} I & II & III \\ IV & V & VI \\ VII & VIII & IX \end{pmatrix}_{(A_0,B_0,C_0)} . \tag{4.12}$$

Here the block I corresponds to the derivation of the functions f with respect to A at (A_0, B_0, C_0) i.e.:

$$I = \frac{\partial f}{\partial A} = \begin{pmatrix} \frac{\partial f_1}{\partial A_1} & \frac{\partial f_1}{\partial A_2} & \cdots & \frac{\partial f_1}{\partial A_K} \\ \frac{\partial f_2}{\partial A_1} & \frac{\partial f_2}{\partial A_2} & \cdots & \frac{\partial f_2}{\partial A_K} \\ \vdots & \vdots & \cdots & \vdots \\ \frac{\partial f_K}{\partial A_1} & \frac{\partial f_K}{\partial A_2} & \cdots & \frac{\partial f_K}{\partial A_K} \end{pmatrix}_{(A_0,B_0,C_0)} . \tag{4.13}$$

In the same way we can express all remaining blocks of the matrix $\mathcal{J}$, (shown below). Computing the corresponding derivatives we obtain that the blocks of the general Jacobian matrix $\mathcal{J}$ associated to the illustrative model within K

compartments are given as:

$$I = \frac{\partial f}{\partial A} = \left(-\frac{2k_1}{h^3}A_0 - k_5\right)\mathbb{I} + \frac{D_a}{h^2}\mathbb{D},$$
$$II = \frac{\partial f}{\partial B} = \left(k_2 + \frac{k_3}{h^3}C_0\right)\mathbb{I}, \qquad III = \frac{\partial f}{\partial C} = \left(\frac{k_3}{h^3}B_0\right)\mathbb{I},$$
$$IV = \frac{\partial g}{\partial A} = \left(\frac{2k_1}{h^3}A_0\right)\mathbb{I}, \qquad V = \frac{\partial g}{\partial B} = --k_2\mathbb{I} + \frac{D_b}{h^2}\mathbb{D},$$
$$VI = \frac{\partial g}{\partial C} = 0 \times \mathbb{I}, \qquad VII = \frac{\partial h}{\partial A} = 0 \times \mathbb{I},$$
$$VIII = \frac{\partial h}{\partial B} = \left(-\frac{k_3}{h^3}C_0\right)\mathbb{I}, \quad IX = \frac{\partial h}{\partial C} = \left(-\frac{k_3}{h^3}B_0\right)\mathbb{I} + \frac{D_c}{h^2}\mathbb{D}.$$

Here $\mathbb{I}$ denotes the identity matrix and $\mathbb{D}$ is given as

$$\mathbb{D} = \begin{pmatrix} -1 & 1 & 0 & 0 & \dots & 0 & 0 & 0 \\ 1 & -2 & 1 & 0 & \dots & 0 & 0 & 0 \\ 0 & 1 & -2 & 1 & \dots & 0 & 0 & 0 \\ \vdots & \vdots & \vdots & \ddots & \ddots & \ddots & \vdots & \vdots \\ 0 & \dots & \dots & \dots & 0 & 1 & -2 & 1 \\ 0 & \dots & \dots & \dots & \dots & 0 & 1 & -1 \end{pmatrix},$$

Knowing the formula for the Jacobian matrix, we can determine the minimal number of compartments by a simple loop:

1. Fix domain size and choose an initial number of compartments, usually $K = 2$.
2. For given K compute the homogeneous steady state defined in (4.11) and the corresponding Jacobian matrix $\mathcal{J}$.
3. Compute the eigenvalues of the matrix $\mathcal{J}$.
4. *If* $Re(\lambda) < 0$ for all eigenvalues λ of the matrix $\mathcal{J}$ *then* set $K = K + 1$ and continue with the step 2. Otherwise go to step 5.
5. *If* at least one of the eigenvalues of matrix J has positive real part, *then* K is the minimal number of compartments and the loop can be stopped.

In the first step of the loop it is possible to use arbitrary K for which we know that the systems does not undergo the Turing instability in $K-1$ compartments. Now consider the illustrative model within domain $[0, 1]$ μm with diffusion coefficients and reaction rates given by $(3.49) - (3.53)$. Then, with the use of the

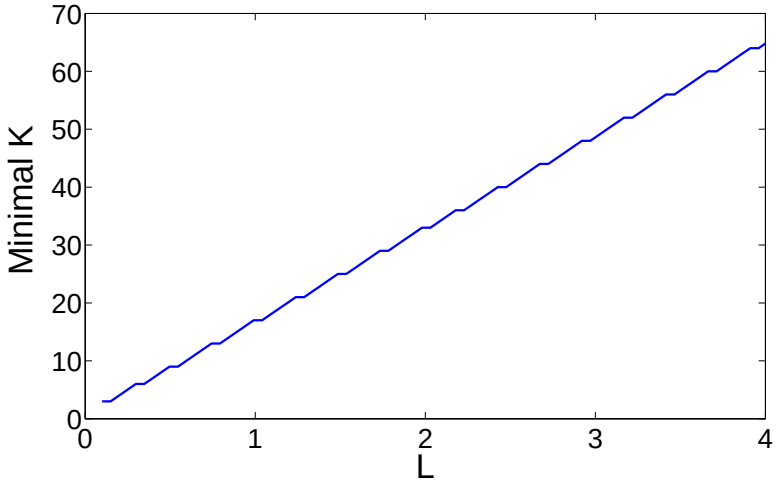

Figure 4.6: *The relation of domain size and minimal number of compartments needed for the Turing instability in the illustrative model. Here L denotes the length of the domain expressed in μm.*

above loop, we find that the minimal number of compartments needed for Turing instability is $K = 17$. In the figure 4.6 we present the relation of the domain size and the minimal number of compartments for the illustrative system. From the figure we can see that this relation is not defined if the domain is too small. This is consistent with the statement from the Chapter 3., where we showed that no Turing patterns are produced if the domain is too small.

Remark. The presented idea for determining the minimal number of compartments can be easily rewrite and used for further systems. For instance, no Turing instability can arise in the Schnakenberg system within the "one dimensional" domain of length $L = 1\ \mu m$ with the diffusion coefficients and reaction rates defined in $(3.54) - (3.56)$ if $K < 7$.

4.3.2 Stochastic Switching Between States of the Illustrative Model

To investigate the role of the noise in the system we will consider the illustrative model in the domain $[0, 1]\ \mu m$ divided into $K = 17$ compartments. The reason why we consider the system with the minimal number of compartments, is that the effect of the noise will be strongest there. Furthermore we will assume that the number of molecules in each compartment is of the order 100. This can be achieved by appropriate rescaling of reaction rates similarly as in (4.10). Let us note that we do not observe switching between different states using this order of molecules in "one dimensional domain" divided into $K = 100$ compartments. Initially we will consider 200 molecules of A, 400 molecules of B and 40 molecules

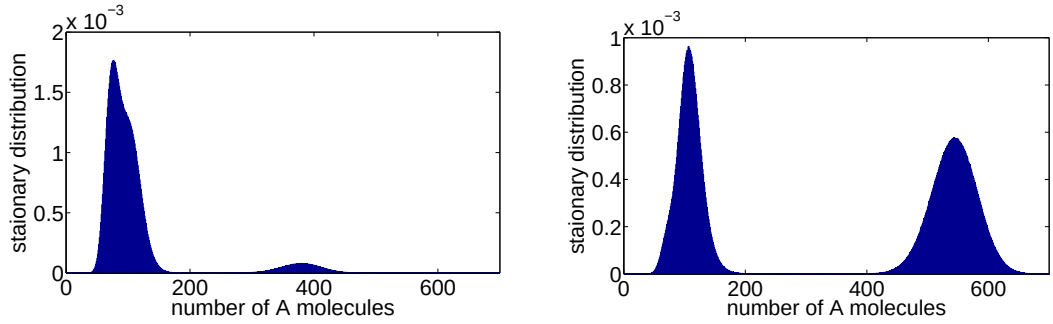

Figure 4.7: *The stationary distributions of A molecules in the first two compartments.*

of C in each compartment, i.e. $A_i(0) = 200$, $B_i(0) = 400$ and $C_i(0) = 40$, where $i = 1, \ldots, 17$. This initial state corresponds to the homogeneous steady state of this system.

To investigate the behaviour of the system we compute the stationary distribution in each compartment. For illustration we plot the stationary distribution of molecules of A in the first two compartments (see the Figure 4.7). The shape of these stationary distributions invokes that as the system evolves it can switch between states with different number of molecules within a single compartment. The result of this switching is a different ordering of patterns over time. This is the first non-deterministic observation, because any pattern rearrangement is possible in the deterministic models.

Furthermore, we would like to know if the noise in this system is strong enough to cause the switching between states with different number of peaks. Thus we would like to know if the number of patterns (peaks) can change in the time. At first we need to define a peak. Since the steady state of A molecules in this system is defined by 200 molecules of A within each compartment we distinguish two different states in each compartment. The first one is the state where the number of A molecules is more then 200 and the second one is the state with less than 200 molecules of A. If the system is out of the steady state and we plot the number of molecules of A in each compartment then peaks will arise in the compartments at the first state and pits in the compartments at the second state. To investigate the switching of the system between states with different number of peaks we define a matrix describing the state of A molecules within all 17 compartments. This matrix will be denote by $\mathbb{S}$ and it will consists of 17 columns, where each column corresponds to one compartment. Each line of the matrix $\mathbb{S}$ will belong to one unit of time. The entrances of this matrix will be only numbers 0 and 1, where 0 stands for the compartments where the number of A molecules is less then 200 and number 1 denotes compartments with more than 200 molecules of A. Thus the matrix $\mathbb{S} = \{s_{ij}\}$, where $j = 1, \ldots, 17$ and i is from the set of

time steps, can be expressed

$$s_{ij} = \begin{cases} 1 & A_j(i) > 200 \\ 0 & A_j(i) < 200 \end{cases} \tag{4.14}$$

It means that each line of $\mathbb{S}$ provides the number and positions of peaks in a given time step.

We simulate the evolution of the illustrative model within 17 compartments for a long time and we store the state of A molecules to the matrix $\mathbb{S}$ each second. In the figure 4.8 we present the evolution within 30000 seconds, where one state of A molecules is plotted every 500 seconds. Thus on the figure 4.8 we plot 60 states, where white color stands for the compartments determined by number one in the matrix $\mathbb{S}$ and black color is for the compartments with number zero. In the figure we can observe oscillations in the peaks ordering. Some of these oscillations are suppressed, but some result in the change in the number of peaks. Looking at right columns in the figure 4.8, we can see a state with nine peaks. This state occurs most often (more then 80% time), however as we can see states with 7 and 8 peaks are also possible.

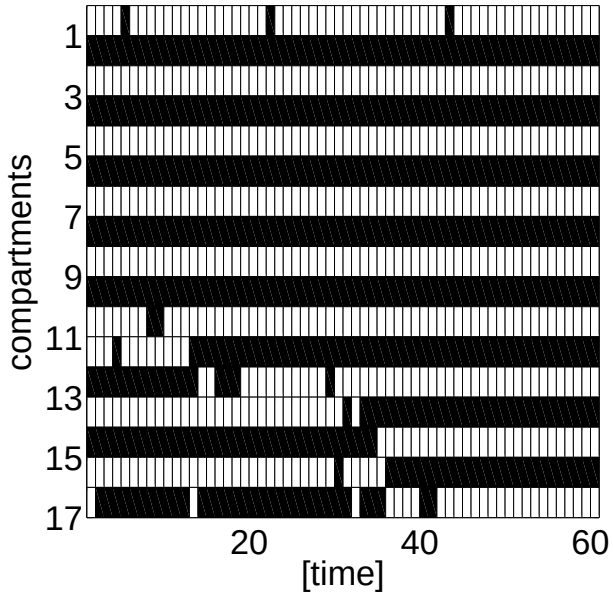

Figure 4.8: *Evolution of the illustrative model in the domain of length $L = 1$ μm divided into 17 compartments. Black color denotes compartments where the number of A molecules is less then 200. Compartments with more than 200 molecules of A are denoted by white color. Each column corresponds to the state of A molecules within one unit of time. For instance the last peak describes the state with nine peaks. The system evolved for 30 000 seconds and we plot the state of A molecules every 500 seconds.*

In the same way we can investigate the states of different systems. For instance, let us consider the Schnakenberg system in domain $[0, 1]\mu m$ divided into $K = 7$ compartments, with reaction rates and diffusion coefficients given in $(3.54) - (3.56)$. We consider the same order of molecules per compartment as in the illustrative model. In the figure 4.9 is the evolution of this system within 40 seconds. The state of A molecules is plotted every second. The transition of the system from the state with four peaks to three peaks can be clearly observed. The switch between states with different number of peaks occurs faster as in the illustrative model, because this model consists only from 7 compartments.

Similar analysis can be done in systems with larger number of compartments. By increasing the number of the compartments the system slowly loose it ability to switch between the states with different number of patterns, however the rearrangement of patterns with the same number of peaks is still possible. Further increase in the number of compartments removes the ability of pattern rearrangements. Which is nothing surprising, because the more compartments we use closer we are to the deterministic case.

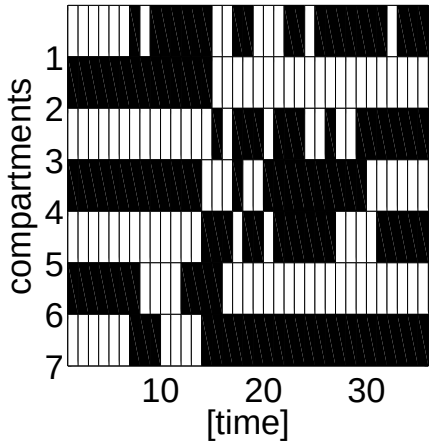

Figure 4.9: *Evolution of the Schnakenberg model in the domain of the length $L = 1$ μm divided into 7 compartments. Black color denotes pits and white color is for peaks. Each column correspond to the state of A molecules within one second. The system evolves for 40 seconds.*

5. Molecular-Based Stochastic Reaction-Diffusion Algorithm

In the previous chapter we studied a model where compartments were used to localize position of molecule in well-mixed system. However, when more precise localisation is desired, one need to proceed to detail models. In this chapter we present Molecular-based models which allow to follow trajectories of individual molecules. Models of this type are used in a number of applications, including modelling of ion channels [56], liquid crystals [57] or gene expression [55]. Moreover, this model can be applied for systems which are not well-mixed. To investigate the trajectories of molecules, we need to consider a different model for molecular diffusion then in the compartment-based model. This is explained in Section 5.1. Then in Section 5.2 we study modelling of different types of chemical reactions. In Section 5.4 we apply the molecular-based model to the illustrative system. Let us note that in the molecular-based algorithm, each molecule is considered as a sphere represented by the position of its center.

5.1 Diffusion in the Molecular-based Model

Molecules as any small particles have a non-zero kinetic energy and a non-zero instantaneous speed [7]. To obtain a better idea how the molecular diffusion looks like, please see attached movie called *diffusion.avi* or download it from *http://tdo.sk/∼ jana/diffusion.avi*. There the molecular diffusion in a cubic domain is presented. Molecules of different chemical species are presented as different coloured dots. As we can see the trajectories of the molecules are not straight, but they execute the Brownian motion. Therefore the position $[X_i(t), Y_i(t), Z_i(t)]$ of the i-th diffusing molecule evolves according to the system of three stochastic differential equations (SDEs) [6]

$$X_i(t + \mathrm{d}\,t) = X_i(t) + \sqrt{2D_i}\,\mathrm{d}\,W_{i,x}, \tag{5.1}$$

$$Y_i(t + \mathrm{d}\,t) = Y_i(t) + \sqrt{2D_i}\,\mathrm{d}\,W_{i,y}, \tag{5.2}$$

$$Z_i(t + \mathrm{d}\,t) = Z_i(t) + \sqrt{2D_i}\,\mathrm{d}\,W_{i,y}, \tag{5.3}$$

where $\mathrm{d}\,W_{i,x}, \mathrm{d}\,W_{i,y}, \mathrm{d}\,W_{i,z}$ are white noises and D_i is the diffusion constant of the i-th particle. To simulate trajectories of the system of SDEs (5.1) – (5.3) we will use the Euler-Maruyama method [54, 58]. It means we choose a small time step

Δt and compute the position of i-th molecule at time $t + \Delta t$ by

$$X_i(t + \Delta t) = X_i(t) + \sqrt{2D_i\Delta t}\,\xi_{i,x}, \tag{5.4}$$
$$Y_i(t + \Delta t) = Y_i(t) + \sqrt{2D_i\Delta t}\,\xi_{i,y}, \tag{5.5}$$
$$Z_i(t + \Delta t) = Z_i(t) + \sqrt{2D_i\Delta t}\,\xi_{i,y}, \tag{5.6}$$

where $\xi_{x,i}, \xi_{y,i}, \xi_{z,i}$ are normally distributed random numbers.
In the following simulations we will consider a system with the reflexive boundary conditions, i.e. whenever a molecule hits the boundary it is reflected back. To explain the implementation of the reflexive boundary conditions to the above diffusion model, let us for simplicity consider the diffusion in one dimensional domain $[0, L]$. It means we assume that molecules diffuse only along the x coordinate. Then the reflexive boundary conditions are implemented as follows [7]:

If $X_i(t + \Delta t)$ computed by (5.4) is less then 0 then
$X_i(t + \Delta t) = -X_i(t) - \sqrt{2D_i\Delta t}\,\xi_{x,i}$.

If $X_i(t + \Delta t)$ computed by (5.4) is greater then L then
$X_i(t + \Delta t) = 2L - X_i(t) - \sqrt{2D_i\Delta t}\,\xi_{x,i}$.

This mirror reflection can be easily extended for the three dimensional domain.

5.2 Modelling of Chemical Reactions by Molecular-based Model

In this section we study modelling of chemical reactions from the illustrative model (2.1) − (2.5). At first we explain modelling of the zero-order and first-order chemical reactions. Then we present Erban and Chapman's $\lambda - \bar{\rho}$ model [6] for second-order reactions and finally we describe the model for reversible chemical reactions.

5.2.1 Zero and First Order Chemical Reactions

To explain the modelling of zero and first order chemical reactions let us consider reactions (2.3) and (2.4) i.e.

$$\emptyset \xrightarrow{k_4} A \quad \text{and} \quad A \xrightarrow{k_5} \emptyset\,.$$

Since both of these reactions occur without molecular collisions, they can be simulated same as in the Gillespie algorithm. It means, the probability that one molecule of A is produced within time interval $[t, t+\mathrm{d}\,t)$ in the domain of volume ν is $k_4\nu\,\mathrm{d}\,t$. The probability that one molecule of A dissociates within time interval $[t, t + \mathrm{d}\,t)$ is $A(t)k_5\,\mathrm{d}\,t$, where $A(t)$ is a number of A molecules in the system at

time t.

To implement these reactions numerically we substitute the infinitesimally small time step dt by finite time step Δt, which needs to be chosen so small that $k_3\nu\Delta t << 1$ and $A(t)k_4\Delta t << 1$. To avoid to this restriction on the small time step Δt we can simulate the production and the dissociation as a Poisson process with the rate constants k_4 and k_5, respectively. It means, the probability that one molecule of A is produced in time interval $[t, t+\Delta t)$ is equal to $1-\exp(-k_3\Delta t)$. Similarly, the probability that one molecule of A dissociates within $[t, t+\Delta t)$ is equal to $1-\exp(-k_4\Delta t)$. Thus the implementation of these reactions is easy for arbitrary time step.

5.2.2 Second Order Reactions

As we already know the second order chemical reactions require collisions of reacting molecules. Since the molecular-based model treats molecules as points, we can assume that two molecules collide, whenever distance of their centres is less than the sum of molecular radii. However, because of the reaction-activation energy, not every molecular collision is necessary followed by the reaction. Moreover in some cases molecules may only react if they collide in a certain way, for instance, if certain "biding sides" on the surface of the molecules meet [22]. To incorporate all of this to the simulation of the second order reaction (2.3), we will use the Erban and Chapman $\lambda-\bar{\rho}$ model [6]. There, it is postulated that a molecule of B and a molecule of C can react with probability P_{λ_3} whenever the distance of their centres is smaller than the reaction radius $\bar{\rho}_3$. The index 3 in the terms $\bar{\rho}_3$ and P_{λ_3} means that this parameters are related to the third reaction from the illustrative model, i.e. to the reaction (2.3). This can be schematically expressed as

$$\text{If } \operatorname{dist}(B,C) \leq \bar{\rho}_3 \;\Rightarrow\; B+C \xrightarrow{k_3} B+A \text{ with probability } P_{\lambda_3}.$$

Thus this model makes use of two parameters P_λ and $\bar{\rho}_3$, while the reaction (2.3) is described in terms of one measurable parameter k_3. To implement the algorithm numerically we need to relate model parameters with the quantity k_3. The formulae relating these parameters is derived in [6]. In order to keep this thesis complete we present this formulae in Theorem 7. For better orientation we inherit the notation presented in [6]. To simplify the derivation of the desired formulae let us define the dimensionless parameters

$$\tilde{\gamma} = \frac{s}{\bar{\rho}_3} = \frac{\sqrt{2(D_B+D_C)\Delta t}}{\bar{\rho}_3}, \qquad \tilde{\kappa} = \frac{k_3\Delta t}{\bar{\rho}_3^3} \quad \text{and} \quad \tilde{\rho} = \frac{\bar{\rho}_3}{\bar{\rho}_3} = 1. \tag{5.7}$$

Here the term s denotes an average change in the relative position of molecule of B and molecule of C during one time step. Moreover we define an auxiliary

function $\tilde{g}(r) : [0, \infty) \to [0, 1]$ as the solution of the integral equation

$$\tilde{g}(r) = (1 - P_{\lambda_3}) \int_0^1 K(r, r'; \tilde{\gamma}) \tilde{g}(r') \, \mathrm{d}\, r' + \int_\infty^1 K(r, r', \tilde{\gamma}) \tilde{g}(r') \, \mathrm{d}\, r', \tag{5.8}$$

satisfying $\tilde{g}(r) \to 1$ as $r \to \infty$. The function $K(z, z', \tilde{\gamma})$ is given by

$$K(z, z', \tilde{\gamma}) = \frac{z'}{z\tilde{\gamma}\sqrt{2\pi}} \left(\exp\left[-\frac{(z - z')^2}{2\tilde{\gamma}^2} \right] - \exp\left[-\frac{(z + z')^2}{2\tilde{\gamma}^2} \right] \right). \tag{5.9}$$

The function $\tilde{g}(r)$ depends on dimensionless parameters P_{λ_3} and $\tilde{\gamma}$ which can be expressed as $\tilde{g}(r) \equiv \tilde{g}(r, P_{\lambda_3}, \tilde{\gamma})$.

Theorem 7. *(Relation of $P_{\lambda_3}, \bar{\rho}_3$ and k_3)*
Let A, B and C be chemical species with diffusion coefficients D_A, D_B and D_C which are subject to the reaction (2.3) *simulated by the $\lambda - \bar{\rho}_3$ model. Then the model parameters P_{λ_3}, $\bar{\rho}_3$ and the rate constant k_3 are related by the following equation*

$$\frac{k_3 \Delta t}{\bar{\rho}_3^3} = P_{\lambda_3} \int_0^1 4\pi r^2 \tilde{g}(r) \, \mathrm{d}\, r. \tag{5.10}$$

The proof of this theorem is presented in [6], Appendix F, or in the Appendix A.2 of this thesis. The formula (5.10) can be considered as follows. Since k_1, D_B and D_C are known, the time step Δt can be specified at the beginning of the simulation, then the equation (5.10) is one equation for two unknowns. Moreover, having the formulae relating P_{λ_3} and $\bar{\rho}_3$, we can choose the reaction radius $\bar{\rho}_3$ close to the molecular radius and use k_3 to compute the appropriate value of P_{λ_3}. The numerical method for solving equation (5.10) is introduced in [6], Appendix F, and it is also presented in the Appendix A.2 of this thesis.

5.2.3 Reversible Chemical Reactions

Let us consider the reversible reaction (2.1). As we mentioned in the Chapter 2, this reaction effectively describes two reactions, the second-order reaction (2.6) and the first-order reaction (2.7). Although, we already know how to simulate these types of reactions, the situation is not so straightforward as it may seem. For illustration, let us assume that the reaction (2.6) is simulated by the $\lambda - \bar{\rho}$ model and that the probability $P_\lambda = 1$. Furthermore assume the cleavage of the complex B is described by the Poisson process with rate k_2. When the molecule B dissociates we introduce two new molecules of A to the system. But, what should be their positions? A natural way to initialise these new molecules is by the position of the complex B which was destroyed during this reaction. However, if the next step of the computer code describes the forward reaction (2.6), then the new molecules of A will immediately create the complex B. They

have to react, because their distance is zero. In particular we may obtain different results by different ordering of the subroutines in the computer code [2, 7]. In our previous work [2] we solved this problem by introducing an extra model parameter called unbinding radius and denoted $\bar{\sigma}$. We assume that whenever the complex B dissociates we introduce new molecules of A with initial separation equal to $\bar{\sigma}$. Then the model for the reversible reaction (2.1) can be summarized as follows. If the distance of two different molecules of A is less then the reaction radius $\bar{\rho}_1$, then the forward reaction (2.6) occurs with the probability P_{λ_1}. The index 1 in $\bar{\rho}_1$ and P_{λ_1} means that these parameters are related to the first reaction from the illustrative model, i.e. to (2.1). On the other hand, the cleavage of the complex B is simulated as a Poisson process with parameter k_2. When the molecule B dissociates we introduce two new molecules of A with the initial separation given by $\bar{\sigma}$.

This model description makes use of three model parameters P_{λ_1}, $\bar{\rho}_1$ and $\bar{\sigma}$, while the reaction (2.1) is described in terms of two parameters k_1 and k_2. Since we already use the parameter k_2 to describe the dissociation of complex B, the remaining parameters P_{λ_1}, $\bar{\rho}_1$ and $\bar{\sigma}$ need to be related to the reaction rate k_1. The derivation of this relation is presented in [2]. In order to keep this thesis complete we present this relation in Theorem 8. Similarly as in the previous section, we firstly define dimensionless parameters

$$\gamma = \frac{\sqrt{4D_A\Delta t}}{\bar{\rho}_1}, \qquad \kappa = \frac{k_1\Delta t}{\bar{\rho}_1^3} \quad \sigma = \frac{\bar{\sigma}}{\bar{\rho}_1} \quad \text{and} \quad \tilde{\rho} = \frac{\bar{\rho}_1}{\bar{\rho}_1} = 1. \tag{5.11}$$

We also define the auxiliary function $g(r) : [0, \infty) \to [0, 1]$ as the solution of the integral equation

$$g(r) = (1 - P_{\lambda_1}) \int_0^1 K(r, r', \gamma) g(r') dr' + \int_1^\infty K(r, r', \gamma) g(r') dr' \tag{5.12}$$

$$+ K(r, \sigma, \gamma) \frac{P_{\lambda_1}}{4\pi\sigma^2} \int_0^1 g(r) 4\pi r^2 dr,$$

satisfying $g(r) \to 1$ as $r \to \infty$, where $K(r, r', \gamma)$ is defined in (5.9). The function $g(r)$ depends on parameters P_{λ_1}, γ and $\bar{\sigma}$, what can be expressed as $g(r) \equiv g(r, P_{\lambda_1}, \gamma, \bar{\rho})$. Let us note the the functions $\tilde{\gamma}$, $\tilde{\kappa}$ and $\tilde{g}$ defined in the previous section are in general different as the function γ, κ, g and P_{λ_1} introduced in this section.

Theorem 8. *(Relation of P_{λ_1}, $\bar{\rho}_1$, $\bar{\sigma}$ and k_1)*
Let A and B be chemical species diffusing with diffusion constants D_A and D_B which are subjects to the reversible reaction (2.1) *simulated by the algorithm presented in this section. Then the model parameters $\bar{\rho}_1$, $\bar{\sigma}$, P_{λ_1} and reaction rate k_1*

are related by the following equation

$$\frac{k_1 \Delta t}{\bar{\rho}_1{}^3} = P_{\lambda_1} \int_0^1 4\pi r^2 g(r) dr. \tag{5.13}$$

The proof of this theorem can be found in [2] and it is also presented in Appendix A.3. Although equation (5.13) has the same form as the equation (5.10) it describes different relation. The formulae (5.13) is one equation for three unknown, P_{λ_1}, $\bar{\rho}_1$ and $\bar{\sigma}$. If we choose $\bar{\rho}_1$ to be close to the molecular radii than equation (5.13) provide the relation between P_{λ_1} and $\bar{\sigma}$. In Appendix A.3 we briefly describe the numerical method for solving equation (5.10) introduced in [2].

5.3 Molecular-based Algorithm for the Illustrative model

In the Section 5.1 we presented simulation of molecular diffusion. Then in the Section 5.2 we explained modelling of each chemical reaction from the illustrative model $(2.1) - (2.5)$. Bringing these models together we obtain a reaction-diffusion molecular-based algorithm for the illustrative system.

THE MOLECULAR BASED ALGORITHM

1. Initialisation: set time $t = 0$, define the domain size, specify the initial number and positions of molecules of each chemical species and define a time step Δt and a stopping time t_{STOP}.

2. For each molecule in the system compute its position in the time $t + \Delta t$ by (5.4)-(5.6). If the computed position is outside the domain, apply the reflexive boundary conditions.

3 . For each molecule of A compute its distance to the remaining A molecules in the system. Whenever this distance is less then the reaction radius $\bar{\rho}_1$, generate a random number r_1 uniformly distributed in the interval $(0, 1)$. If $r_1 < P_{\lambda_1}$, then remove both reacted molecules of A and introduce a new molecule of B. Initialise the position of B at the halfway between the reactants.

4. For each molecule of B generate a random number r_2 uniformly distributed in the interval (0,1). If $r_2 < (1 - \exp(-k_2\Delta t))$ then introduce two molecules of A to the system. Place them at distance $\bar{\sigma}$ apart so that their centre of mass is equal to the position of complex B before it dissociate. Consequently remove the reacted complex B.

5. For each molecule of B compute its distance to each molecule of C. Whenever this distance is less then the reaction radius $\bar{\rho}_3$ generate a random number r_3 uniformly distributed in the interval $(0, 1)$. When $r_3 < P_{\lambda_3}$ introduce one molecule of A and place it at the position of reacted molecule of C. Consequently remove this C molecule.

6. Generate a random number r_4 uniformly distributed in the interval $(0, 1)$. If $r_4 < (1 - \exp(-k_4\Delta t))$ then introduce one molecule of A at a random place in the system.

7. For each molecule A generate a random number r_5 uniformly distributed in the interval $(0, 1)$. If $r_5 < (1 - \exp(-k_5\Delta t))$ then remove the molecule of A from the system.

8. Generate a random number r_6 uniformly distributed in the interval $(0, 1)$. If $r_6 < (1 - \exp(-k_6\Delta t))$ then introduce one molecule of C at a random place in the system.

9. Set $t = t + \Delta t$ and continue with the step 2 until t reaches the t_{STOP}.

The second step in the algorithm models diffusion of molecules. The step 3. describes the forward reaction (2.6) and the step 4. the backward (2.7) from the

chemical reaction (2.1). The steps 5.-8. simulate the remaining reactions from the illustrative model in the same order as they are presented in $(2.2) - (2.5)$.

5.4 Realisation of the Molecular-Based SSA

Using the molecular-based approach we can determine the positions of all molecules in every unit of time. On the other hand, the price that we need to pay for such detail system description is a high computational intensity. Moreover this algorithm was proposed for systems with small number of molecules. Therefore its application to systems with more than a few hundred molecules is impractical. Therefore in order to investigate pattern formation mechanisms in the illustrative model simulated by molecular-based algorithm, we consider two simplifications. At first, we will use much smaller domain as in the previous chapters. We consider elongate domain $[0, L]\times[0, h]\times[0, h]$ and the "square" domain $[0, L]\times[0, L]\times[0, h]$, where $L = 0.1\ \mu m$ and $h = 0.01\ \mu m$. Although this domain is significantly smaller, it is still large enough to observe pattern formation.
Secondly, we will assume the $P_{\lambda_1} = 1$ and $P_{\lambda_3} = 1$. Thanks to this we do not need to generate random numbers in the steps 3. and 5. of the molecular-base algorithm. Moreover, in this specific situation we can use a reaction-diffusion simulator called Smoldyn [34, 35, 36]. It was created by S. Andrew in 2004 and is available for free at *http://www.smoldyn.org/download.html*. Smoldyn can simulate chemical reactions up to second-order, including reversible reactions. The algorithms for chemical reactions implemented in Smoldyn are similar as those presented in Section 5.2, however in the second-order chemical reactions the probability P_λ is always equal to one in Smoldyn. A disadvantage of this choice of probability is that the reaction radius is, for typical values of the biomolecular rate constants and diffusion coefficients, unrealistically small compared to the size of individual molecules [6]. However this is not the case of the illustrative model.

Finally we can proceed to the simulation of the illustrative model. We use the reaction rates and the diffusion coefficients given in $(3.49) - (3.53)$. We choose the time step $\Delta t = 10^{-7} sec$. According to our assumption the probability $P_{\lambda_3} = 1$. Then we can use the equation (5.10) or Smoldyn simulator to compute that the corresponding reaction radius is $\bar{\rho}_3 = 1.69 \times 10^{-5}\ \mu m$. Similarly, for $P_{\lambda_1} = 1$ we can use Smoldyn to compute that $\bar{\rho}_1 = 6.71 \times 10^{-5}\ \mu m$ and $\bar{\sigma} = 0.0003\ \mu m$. Or we can use (5.10) to compute $\bar{\rho}_1$ corresponding to P_{λ_1}. Then we use equation (5.13) to find $\bar{\sigma}$. Initially we consider 100 molecules of each chemical species randomly distributed in the system. At first we consider the evolution of the system in the elongate domain $[0, L] \times [0, h] \times [0, h]$, where $L = 0.1\ \mu m$ and $h = 0.01\ \mu m$. In Figure 5.1a we plot positions of B molecules after 500 seconds

of the simulation. Each dot corresponds to one molecule. In order to compare this result with compartment-based model, we divide the computational domain in 10 compartments (see Figure 5.1a). This domain division corresponds to the division in Chapter 4, where we used 100 compartments for the domain of length 1 μm. To observe pattern formation, we compute the number of molecules in each compartment. In Figure 5.1b we plot the number of B molecules in each compartment.

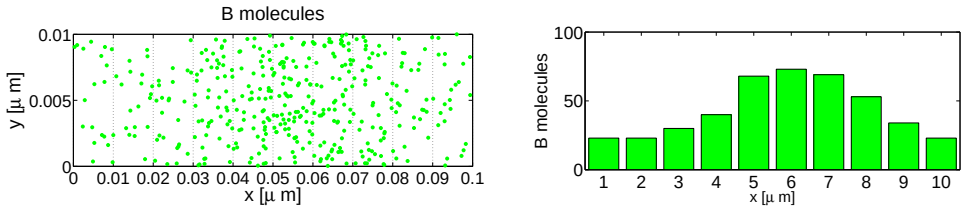

(a) (b)

Figure 5.1: *Molecules of B after* 500 *seconds of simulation. In (a) we plot positions of B molecules. Each dot corresponds to one molecule of B in the system. For the reason of comparison with the compartment-based model, we divide the computational domain in imaginary compartments, presented in (a). In (b) we plot number of molecules in each compartment.*

Similarly we proceed in the "square domain" $[0, L] \times [0, L] \times [0, h]$, where $L = 0.1$ μm and $h = 0.01$ μm. We let the system evolves for 400 seconds. At the end of the simulation we divide the domain in 10×10 compartment and compute the number of B molecules in each compartment. In Figure 5.2 we present the number of B molecules computed by the molecular based model in the comparison with the deterministic solution computed in the same domain. In the Figure 5.2, we can observe the formation of a pattern, however it is obvious that the molecular-based simulation needs to evolve much more longer in order to obtain better result.

Due to the high computational intensity of the molecular-based model, we do not investigate the behaviour of the system in the deterministic limit, i.e. in the situation with a large number of molecules. However this model allows us to observe the stochastic behaviour. Although the considered domain is too small and thus cannot produce states with different number of peaks, the states with different formation of a peak can be observed. In Figure 5.3 we present number of B molecules, computed by the molecular based model, in different times. Initially we consider 100 molecules of each chemical species randomly distributed in the system. We again divide the domain in 10 imaginary compartments and compute the number of molecules in each compartment.

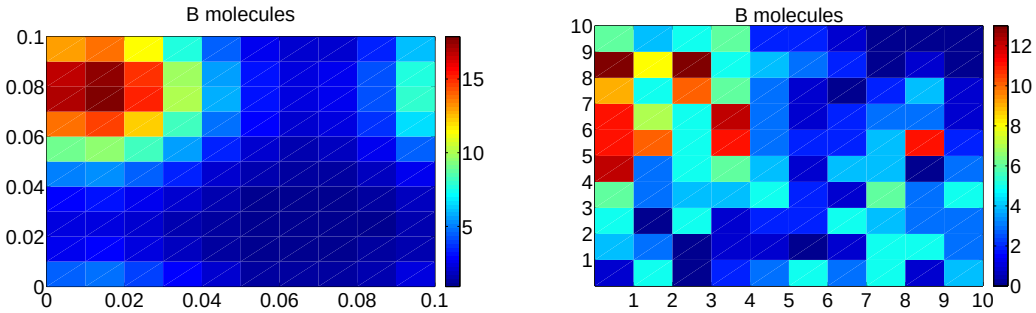

(a) (b)

Figure 5.2: *Number of B molecules computed by molecular-based model (b) in the comparison with the deterministic solution (a).*

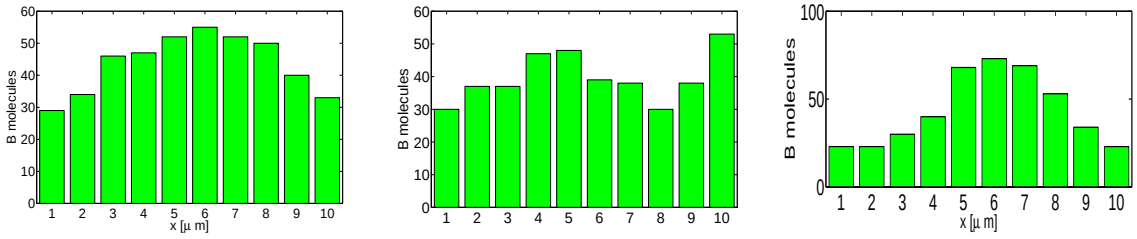

(a) (b) (c)

Figure 5.3: *States with different formation of a peak. In (a) we plot number of B molecules for time $t = 150$ seconds, in (b) for time $t = 300$ seconds and in (c) for time $t = 500$ seconds of the simulation.*

Remark. The main advantage of the molecular-based model is detailed description. Moreover it can be applied also for systems which are not well-mixed. However all currently known molecular-based models are proposed for maximum second order chemical reactions and bimolecular reversible reactions [2]. On the other hand each chemical reaction of the third and higher order can be simulated as a system of first and second order reactions [1]. For instance, the first reaction in the Schnakenberg model $2A + C \xrightarrow{k} 3A$, can be rewrited as the system of three chemical reactions:

$$\begin{aligned} A + A &\xrightarrow{m_1} B, \\ B + C &\xrightarrow{m_2} B + A, \\ B &\xrightarrow{m_3} A + A, \end{aligned}$$

Thus after appropriate approximation of model parameters (see Section 3.4.2) each chemical reaction can be simulated by the molecular-based algorithm.

6. Summary

In this thesis we studied the reaction-diffusion mechanism related to the formation of Turing patterns. We presented necessary and sufficient conditions under which Turing instability occur. Moreover, for the illustrative model, we derived a complete set of conditions needed for the formation of Turing patterns. Then we investigated the behaviour of Turing patterns with the use the deterministic approach. We showed that even a small change in the initial conditions may lead to a solution with different number of patterns. However, in the deterministic approach, once the state with a given number of patterns is reached, the system stays there. Then we introduced the compartment-based SSA. We showed that in the systems with a large number of molecules this algorithm provides the same results as the deterministic model. Moreover, this model allowed us to observe non-deterministic behaviour in systems with a lower number of molecules. The stochastic switching between states with different ordering of patterns was presented. Then we introduced the molecular-based SSA. This algorithm also describes the rearrangement of patterns in the time. The high computational intensity of this algorithm did not allowed us to investigate the behaviour of the system in the deterministic limit, i.e. in the case with a large number of molecules. Thus as a future work and the progress in the problematic we suggest to find methods decreasing the computational intensity of the molecular-based SSA. An improvement can be probably achieved by parallel programming methods.

In this thesis we focused on reaction-diffusion mechanisms that are present in biological systems. However we would like to point out that presented techniques are not limited to biological applications. Recent advances in astrochemistry have shown that large molecules (commonly called 'space dust') exist in the interstellar medium, and that chemical reactions to form organic compounds can occur on the surface of these dust grains when atoms collide. Since the number of atoms is miniscule, deterministic models derived are quite unsuitable, and Charnley and Rodgers [60, 26] have used the Gillespie algorithm to solve the chemical master equation to calculate abundance of certain hydrocarbons on dust grains.

A. Appendix

A.1 Roots of the polynomial y

Let us consider the polynomial defined in the condition 6) of the theorem 5 in Chapter 3, i.e.

$$y = Am^3 + Bm^2 + Cm + D,$$

where $m = k^2$. Then the roots of this polynomial are given by:

$$\begin{aligned}
m_1 =& -\frac{B}{3A} - \\
&- \frac{1}{3A}\sqrt[3]{\tfrac{1}{2}\left[2B^3 - 9ABC + 27A^2D + \sqrt{(2B^3 - 9ABC + 27A^2D)^2 - 4\,(B^2 - 3AC)^3}\right]} - \\
&- \frac{1}{3A}\sqrt[3]{\tfrac{1}{2}\left[2B^3 - 9ABC + 27A^2D - \sqrt{(2B^3 - 9ABC + 27A^2D)^2 - 4\,(B^2 - 3AC)^3}\right]} \\
m_2 =& -\frac{B}{3A} + \\
&+ \frac{1 + i\sqrt{3}}{6A}\sqrt[3]{\tfrac{1}{2}\left[2B^3 - 9ABC + 27A^2D + \sqrt{(2B^3 - 9ABC + 27A^2D)^2 - 4\,(B^2 - 3AC)^3}\right]} + \\
&+ \frac{1 - i\sqrt{3}}{6A}\sqrt[3]{\tfrac{1}{2}\left[2B^3 - 9ABC + 27A^2D - \sqrt{(2B^3 - 9ABC + 27A^2D)^2 - 4\,(B^2 - 3AC)^3}\right]} \\
m_3 =& -\frac{B}{3A} + \\
&+ \frac{1 - i\sqrt{3}}{6A}\sqrt[3]{\tfrac{1}{2}\left[2B^3 - 9ABC + 27A^2D + \sqrt{(2B^3 - 9ABC + 27A^2D)^2 - 4\,(B^2 - 3AC)^3}\right]} + \\
&+ \frac{1 + i\sqrt{3}}{6A}\sqrt[3]{\tfrac{1}{2}\left[2B^3 - 9ABC + 27A^2D - \sqrt{(2B^3 - 9ABC + 27A^2D)^2 - 4\,(B^2 - 3AC)^3}\right]}
\end{aligned}$$

A.2 Proof of the Theorem 7

However the following derivation of equation (5.10) is reproduced from [6], we present it this thesis in order to keep the $\lambda - \bar{\rho}$ algorithm complete.
Let $c_i(r)$ be the concentration of molecules of B at distance r from the origin. Assuming that molecules of B only diffuse, their concentration at point r after the time interval Δt is given as

$$\int_0^\infty K(r, r', \tilde{\gamma}) c_i(r')\,\mathrm{d}\,r' \tag{A.1}$$

where $K(r, r', \tilde{\gamma})$ is given by (5.9). Let us assume that the particles are removed, in the circle of radius $\bar{\rho}_3$ and centred at origin, with probability P_{λ_3}, and then

diffuse for time Δt. Then (A.1) is modified to

$$c_{i+1}(r) = (1 - P_{\lambda_3}) \int_0^1 K(r, r', \tilde{\gamma}) c_i(r') \,\mathrm{d}\, r' + \int_1^\infty K(r, r', \tilde{\gamma}) c_i(r') \,\mathrm{d}\, r' \qquad \text{(A.2)}$$

Equation (5.8) is an equation for the fixed point of this iterative scheme. The rate of removal of particles (at steady state) during one time step is given by the right hand side of (5.10). Comparing with $\tilde{\kappa}$, we obtain (5.10).
To solve (5.8) , we will use the condition $\tilde{g}(r) \to 1$ as $r \to \infty$. Choosing S large, we can approximate $\tilde{g}(r) = 1$ for $r \geq S$. Let N_1 and N_2 be positive integers. We consider the mesh $r_j = j/N_1$, for $j = 1, 2, \ldots, N_1$ and $r_j = 1 + (S-1)(j - N_1)/N_2$, for $j = N_1 + 1, \ldots, N_1 + N_2$. We discretize (5.8) as

$$\tilde{g}(r_i) = \frac{1 - P_{\lambda_3}}{N_1} \sum_{j=1}^{N_1} K(r_i, r'_j, \tilde{\gamma}) + \frac{S-1}{N_2} \sum_{j=N_1}^{N_1+N_2} K(r_i, r'_j, \tilde{\gamma}) \tilde{g}(r_j) + \int_S^\infty K(r_i, r', \tilde{\gamma}) \,\mathrm{d}\, r'.$$

This is a linear system for $\tilde{g}(r_i)$, $i = 1, 2, \ldots, N_1 + N_2$, which can be solved, for example, by Gaussian elimination.

A.3 Proof of the Theorem 8

In order to keep the algorithm for the reversible reactions complete, let us derive the equation (5.13) according to the approach presented in [2]. At first we rewrite the Theorem 8 in terms of three chemical species A, B and C. This has no impact on the derivation of formulae (5.13), but it allowed us to distinguish between reacting molecules in the system.

Theorem 9. *(Relation of of $\bar{\rho}$, $\bar{\sigma}$, P_λ and k_1)*
Let A, B and C be chemical species diffusing with diffusion constants D_A, D_B and D_C which are subjects to the reversible reaction

$$A + B \underset{k_2}{\overset{k_1}{\rightleftarrows}} C$$

Then the model parameters $\bar{\rho}$, $\bar{\sigma}$, P_λ and the rate constant k_1 are related by following equation

$$\frac{k_1 \Delta t}{\bar{\rho}^{\,3}} = P_\lambda \int_0^1 4\pi z^2 g(z) dz. \qquad \text{(A.3)}$$

Proof. The λ-$\bar{\rho}$ model of the forward chemical reaction $A + B \xrightarrow{k_1} C$ states that molecules of A and molecules of B diffuse with the diffusion constants D_A and D_B, respectively. If the distance between molecule of A and molecule of B is less than $\bar{\rho}$, then the molecules react with the probability P_λ. Let us assume that all molecules of B are centered at the origin. Considering a frame of reference

situated in the molecules of B, we can equivalently describe this process as the random walk of molecules of A which have the diffusion constant $D_A + D_B$. These molecules diffuse to the ball of radius $\bar{\rho}$ (centered at origin) which removes molecules of A with the probability P_λ [6]. In this frame of reference, the reverse step $C \xrightarrow{k_2} A + B$ corresponds to the introduction of new molecules of A at the distance $\bar{\sigma}$ from the origin. Let $c_i(r)$ be the concentration of molecules of A at the distance r from the origin (i.e from the molecules of B). To describe the model for reversible reaction from the numerical point we will consider that the reactions occur first and then the diffusion. It can be schematically expressed as follows

$$c_i(r) \xrightarrow{R} \widetilde{c}_i(r) \xrightarrow{D} c_{i+1}(r),$$

where $\widetilde{c}_i(r)$ is a concentration at the distance r from the origin modified by reaction R (i.e $A + B \underset{k_2}{\overset{k_1}{\rightleftarrows}} C$) and $c_{i+1}(r)$ is a concentration at the distance r from the origin modified by reaction R and then by diffusion D.
Reaction includes removing of the particles of A, in the circle of radius $\bar{\rho}$ and centered at the origin, with probability P_λ and also introducing of particles of A at the distance $\bar{\sigma}$ from the origin. Thus $\widetilde{c}_i(r)$ can be expressed as

$$\widetilde{c}_i(r) = (1 - P_\lambda)\chi_{[0,1]}c_i(r) + \chi_{(1,\infty)}c_i(r) + \omega\delta(r - \bar{\sigma}), \tag{A.4}$$

where ω is a constant describing the production of molecules of A in one time step. Diffusion now implies that

$$c_{i+1}(r) = \int_0^\infty K(r, r', \gamma)\widetilde{c}_i(r')dr', \tag{A.5}$$

where $K(r, r', \gamma)$ is defined in (5.9).
Substituting $\widetilde{c}_i(r)$ in (A.5) we obtain

$$c_{i+1}(r) = (1-P_\lambda)\int_0^1 K(r, r', \gamma)(c_i)(r')dr' + \int_1^\infty K(r, r', \gamma)(c_i)(r')dr' + \omega K(r, \bar{\sigma}, \gamma).$$

Let us assume that $g(r)$ is a fixed point of the iterative scheme (A.5) i.e

$$g(r) = \int_0^\infty K(r, r', \gamma)\widetilde{g}(r')dr',$$

where

$$\widetilde{g}(r) = (1 - P_\lambda)\chi_{[0,1]}g(r) + \chi_{(1,\infty)}g(r) + \omega\delta(r - \bar{\sigma}).$$

For the derivation of the constant ω we use the condition that the diffusion doesn't change the total quantity. This implies that

$$\int_0^\infty g(r)4\pi r^2 dr = \int_0^\infty \widetilde{g}(r)4\pi r^2 dr,$$

and using this we find

$$\omega = \frac{P_\lambda}{4\pi\bar{\sigma}^2}\int_0^1 g(r)4\pi r^2 dr.$$

Consequently

$$g(r) = (1 - P_\lambda) \int_0^1 K(r, r', \gamma) g(r') dr' + \int_1^\infty K(r, r', \gamma) g(r') dr' \tag{A.6}$$

$$+ K(r, \sigma, \gamma) \frac{P_\lambda}{4\pi\bar{\sigma}^2} \int_0^1 g(r) 4\pi r^2 dr.$$

Then the rate of removing particles during one time step is given by

$$\kappa = P_\lambda \int_0^1 4\pi r^2 g(r) dr \tag{A.7}$$

what is the desired relation. □

To solve the equation (A.6) we can use the same numerical approach as is presented in Appendix A.2

Bibliography

[1] J. D. Murray, *Mathematical Biology*, Springer Verlag, (2002).

[2] J. Lipkova, K. Zygalakis, J. Chapman and R. Erban, *Analysis of Brownian Dynamics Simulations of Reversible Bimolecular Reactions*, SIAM Journal on Applied Mathematics, Volume 71, Number 3, pp. 714-730 (2011).

[3] K.Lin, S.G. Schirmer, E. T. C. Wirkus, *Chemical Pattern Formation in Reaction-Diffusion Systems*, (1992).

[4] J. E. Pearson, Science 261, 189 (1993).

[5] R. Erban and J. Chapman,*Reactive boundary conditions for stochastic simulations of reactiondiffusion processes,* Physical Biology 4(1): pp. 16-28 (2007).

[6] R. Erban and J. Chapman, *Stochastic modelling of reaction-diffusion processes: algorithms for bimolecular reactions*, Physical Biology 6(4): 046001 (2009).

[7] R. Erban and J. Chapman,*Stochastic modelling of reaction-diffusion processes*, (2009).

[8] D. Gillespie, Journal of Chemical Physics (2001).

[9] M. Howard and D. Rutenberg, Physics Review Letters 90(12): 128102 (2003).

[10] A. Turing, Phil. Trans. of the Royal Soc. of London 237 (641), pp. 37-72 (1952)

[11] R. E. Baker, *Mathematical Biology and Ecology Lecture Notes*, (2010)

[12] S. Sick, S. Reinker, J. Timmer, T. Schlake, *WNT and DKK determine hair follicle spacing through a reaction-diffusion mechanism*, Science 314, 14471450, (2006).

[13] K. Takahashi, S. Tânase-Nicola, P.R. Wolde, *Spatio-temporal correlations can drastically change the response of a MAPK pathway*, PNAS, vol. 107, no. 6, pp. 2473–2478, (2010).

[14] R.J. Orton, O.E. Sturm, V. Vyshemirsky, M. Calder, D.R. Gilbert, W. Kolch, *Computational modelling of the receptor-tyrosine-kinase-activated MAPK pathway*, The Biochemical Journal, 392, pp. 249–261, (2005).

[15] K. Lipkow, S. S. Andrews and D. Bray, *Simulated Diffusion of Phosphorylated CheY through the Cytoplasm of Escherichia coli*, JOURNAL OF BACTERIOLOGY, pp. 45–53, (2005).

[16] D. Fange and J. Elf, *Noise-Induced Min Phenotypes in E. coli*, PLoS Comp. Biol. (2006)

[17] S, Kondo and R, Asai, *A reaction–diffusion wave on the skin of the marine angelfish Pomacanthus*, NATURE, vol 376, pp. 765 - 768.

[18] T. Erdmann, M. Howard and P.R. ten Wolde, *Role of Spatial Averaging in the Precision of Gene Expression Patterns*, PHYSICAL REVIEW LETTERS, 103, 258101, (2009).

[19] M. Affolter, R. Zeller and E. Caussinus, *Tissue remodelling through branching morphogenesis.*, Nat Rev Mol Cell Biol., 10(12) pp.831-42, (2009).

[20] J. A. Izaguirre, R. Chaturvedi, C. Huang, T. Cickovski, J. Coffland, G. Thomas, G. Forgacs, M. Alber, G. Hentschel, S. A. Newman, et al., *Bioinformatics* 20, 1129 (2004).

[21] E. Zauderer, *Partial Differential Equations of Applied Mathematics*, John Wiley Sons, (1983).

[22] B. Alberts, A. Johnson, J. Lewis, M. Raff, K. Roberts, and P. Walter, *Molecular Biology of the Cell*, Garland Science, New York, (2002).

[23] J. Hattne, D. Fange, and J. Elf, *Stochastic reaction-diffusion simulation with MesoRD*, Bioinformatics 21, no. 12, 2923–2924, (2005).

[24] S. Andrews and D. Bray, *Stochastic simulation of chemical reactions with spatial resolution and single molecule detail*, Physical Biology 1, 137–151, (2004).

[25] D. Gillespie,*A General Method for Numerically Simulating the Stochastic Time Evolution of Coupled Chemical Reactions* JOURNA OF COMPUTATIONAL PHYSICS, (1976), pp. 403-434.

[26] A. Twomey, *On the Stochastic Modelling of Reaction-Diffusion Processes*, (2007), master thesis.

[27] A. M. Turing, *The Chemical Basis of Morphogenesis*, Phil. Trans. R. Soc. London B237, pp.37-72, (1952).

[28] M.Mansour, *A Simple Proof of the Routh-Hurwitz Criterion*, Swiss Federal Institute of Technology, (1988).

[29] R. A. Satnoianu, M. Menzinger and P. K. Maini, *Turing instabilities in general systems*, Springer Verlag, (2000).

[30] R. Descartes, *The Geometry of Rene Descartes with a Facsimile of the First Edition* (trans. D. E. Smith and M. L. Latham),Dover, New York, 1954.

[31] Xiaoshen Wang, *A Simple Proof of Descartes's Rule of Signs*, The American Mathematical Monthly, Vol. 111, No. 6 (2004), pp. 525-526

[32] Crampin, E. J, *Reaction-diffusion patterns on growing domains*, DPhil thesis, University of Oxford, UK, (2000)

[33] K.Lin, S.G. Schirmer, E. T. C. Wirkus, *Chemical Pattern Formation in Reaction-Diffusion Systems*, (1992).

[34] Andrews, Steven S., Nathan J. Addy, Roger Brent, and Adam P. Arkin *Detailed simulations of cell biology with Smoldyn 2.1* PLoS Comp. Biol. 6:e1000705, 2010.

[35] Andrews, Steven S. *Smoldyn Users Manual* http://www.smoldyn.org, 2010.

[36] Andrews, Steven S. *Spatial and stochastic cellular modeling with the Smoldyn simulator* Methods for Molecular Biology, in press, 2010.

[37] N. van Kampen: Stochastic Processes in Physics and Chemistry (1981).

[38] D. Gillespie, Journal of Chemical Physics (2001).

[39] M. Howard and D. Rutenberg, Physics Review Letters 90(12): 128102 (2003).

[40] Ander M, Beltrao P, Di Ventura B, Ferkinghoff-Borg J, Foglierini M, Kaplan A, Lemerle C, Tomás-Oliveira I, Serrano L: *SmartCell, a framework to simulate cellular processes that combines stochastic approximation with diffusion and localisation: analysis of simple networks.* Syst. Biol., Volume 1, Issue 1, p.129–138 (2004).

[41] Steven A. Orszag, *Numerical Methods for the Simulation of Turbulence*, Phys. Fluids Supp. II, 12, 250-257, (1969).

[42] S. Isaacson and C. Peskin, *Incorporating diffusion in complex geometries into stochastic chemical kinetics simulations*, SIAM Journal on Scientific Computing 28, no. 1, 47–74, (2006).

[43] S. Engblom, L. Ferm, A. Hellander, and P. Lotstedt, *Simulation of stochastic reaction-diffusion processes on unstructured meshes*, Technical Report 2008-012, Dept of Information Technology, Uppsala University, Uppsala, Sweden, 2008.

[44] T.E. Woolley, R.E. Baker, E.A. Gaffney and P.K. Maini, *Power spectra method for a stochastic description of diffusion on deterministically growing domain*, In review.

[45] M.A. Gibson and J. Bruck, *Efficient Exact Stochastic Simulation of Chemical Systems with Many Species and Many Channels*

[46] Johan Elf, David Fange, Johan Hattne, *MesoRD User's Guide*, (2011).

[47] Radek Erban Hans Othmer, *From individual to collective behavior in bacterial chemotaxis*, SIAM Journal on Applied Mathematics,Volume 65, Number 2, pp. 361-391 (2004)

[48] Radek Erban and Hans Othmer, *From signal transduction to spatial pattern formation in E.coli: A paradigm for multi-scale modeling in biology*, Multiscale Modeling and Simulation, Volume 3, Number 2, pp. 362-394 (2005)

[49] G. Da Prato and J. Zabczyk, *Ergodicity for Infinite Dimensional Systems*, Cambridge Univ. Press, Cambridge, (1996).

[50] S. Cerrai, *Second Order PDEs in Finite and Infinite Dimensions*, LNM 1762, Springer, (2001).

[51] R. Manthey and B. Maslowski, *A random continuous model for two interacting populations*, Appl. Math.Optim. 45(2002), 213-236.

[52] Lockshin, RA and Williams, CM (1964). *Programmed cell death. II. Endocrine potentiation of the breakdown of the intersegmental muscles of silkmoths*, J Insect Physiol 10: 643-649.

[53] L. Qiao, R. Erban, C. T. Kelley, I.G. Kevrekidis, *Spatially Distributed Stochasic Systems: equation-free and equation-assisted preconditioned computation*, Journal of Chemical Physics, 125, p.204108,(2006).

[54] R. Erban, S. J. Chapman, and P. Maini, *A practical guide to stochastic simulations of reaction-diffusion processes*, 35 pages, available as http://arxiv.org/abs/0704.1908 (2007).

[55] J.S. van Zon and P. R. ten Wolde, *Simlating Biochemical Networks at the Particle Level and in Time and Space: Green's Function Reaction Dynamics*, Physical Review Letters, 128103, (2005).

[56] B. Corry, S. Kuyucak, and S. Chung, *Test of continuum theories as models of ion channels.* II. Poisson-Nernst-Planck theory versu Brownian dynamics, Biophysical Journal, 78 (2000), pp. 2364–2381.

[57] C. Siettos, M. Graham, and I. Kevrekidis, *Coarse Brownian dynamics for nematic liquid crystals: Bifurcation, projective integration, and control via stochastic simulation*, Journal of Chemical Physics, 118 (2003), pp. 10149–10156.

[58] E. Platen, *An introduction to numerical methods for stochastic differential equations*, Acta Numerica, 8 (1999), pp. 197–246.

[59] M. Smoluchowski, *Versuch einer mathematischen Theorie der Koagulationskinetik kolloider Lösungen*, Zeitschrift für physikalische Chemie 92 (1917), 129168

[60] Charnley, S., and Rodgers, S. Pathways to molecular complexity. In Astrochemistry: Recent Successes and Current Challenges (2005), no. 231, International Astronomical Union, pp. 237–246. IAU Symposium.

[61] J. Schnackenberg. *Simple chemical reaction systems with limit cycle behavior.* J. Theor. Biology, 81:389–400, 1979.

Acronyms

SSA ... stochastic simmulation algorithm

PDE ... partial differentila equation

ODE ... ordidnary diffenerantialy equation

D ... diffusion coefficient

k ... reaction rate

L ... length of the domain

K ... number of compartments

h ... size of the compartment

$\bar{\rho}$ ... reaction radius

$\bar{\sigma}$ ... initial separation

P_α ... probability of reaction

Attachments

1. . . . Turing.avi (movie)
2. . . . diffusion.avi (movie)